
HOKKAIDO UNIVERSITY

Title	Rehabilitation of corrosion damaged reinforced concrete beams with recycled nylon fiber reinforced sprayed polymer cement mortar
Author(s)	Orasutthikul, Shanya
Citation	北海道大学. 博士(工学) 甲第12905号
Issue Date	2017-09-25
DOI	10.14943/doctoral.k12905
Doc URL	http://hdl.handle.net/2115/70617
Type	theses (doctoral)
File Information	Orasutthikul_Shanya.pdf


Instructions for use

Hokkaido University Collection of Scholarly and Academic Papers : HUSCAP

REHABILITATION OF CORROSION DAMAGED REINFORCED CONCRETE BEAMS WITH RECYCLED NYLON FIBER REINFORCED SPRAYED POLYMER CEMENT MORTAR

リサイクルナイロン繊維を混入したポリマーセメントモルタルによる
コンクリート部材の補修効果

Shanya Orasutthikul

A THESIS SUBMITTED IN PARTIAL FULFILLMENT OF THE REQUIREMENTS FOR THE DEGREE OF DOCTOR OF PHILOSOPHY

Examination Committee
Prof. Hiroshi Yokota
Prof. Tamon Ueda
Prof. Takafumi Sugiyama

DIVISION OF ENGINEERING AND POLICY FOR SUSTAINABLE ENVIRONMENT

GRADUATE SCHOOL OF ENGINEERING

HOKKAIDO UNIVERSITY

September, 2017

ABSTRACT

In recent decades, the world has been suffering from the dumping of wastes, especially plastics left in seas and oceans. Waste fishing nets account for some of these wastes: 640,000 tons of fishing nets are disposed of in the ocean annually. As the nets become totally entangled, separating them for disposal is impractical. These nets can be harmful to marine life, such as turtles, seals, and other marine mammals, which can become entangled and suffer injury or drowning. In addition, the marine food web could be disrupted. As abandoned nets and plastic garbage tend to gather at or near the surface of seas and oceans, they keep sunlight from reaching small creatures such as planktons and algae. Therefore, the animals that feed on these small creatures are also directly affected. Although the storage of such nets has not caused a serious safety hazard to date, it is important to find suitable recycling solutions. Therefore, it is important and urgent to find suitable way to recycle them.

In the first stage, the author discussed the utilization of recycle waste fishing nets in fiber reinforced mortar. Experimental test results compared the mechanical properties of such mortar made with recycled (R-) nylon fiber to those of such mortar made with recycled polyethylene terephthalate (PET) and polyvinyl alcohol (PVA) short fibers. Two types of R-nylon fiber were investigated: straight fiber and fiber with a knot at each end. The straight R-nylon fibers were obtained by manually cutting waste fishing nets to the lengths of 20 mm, 30 mm, and 40 mm, and adding them to mortar at the volume ratios of 1.0%, 1.5%, and 2.0%. The 40-mm-long knotted fibers were added to mortar at the volume ratios of 0.5%, 0.75%, and 1.0%. The addition of R-nylon fibers improves first-crack strength more than that PVA fibers do. However, the compressive strength decreases with increase in fiber fraction, and decreases with increase in fiber aspect ratio.

In the second stage, the author discussed whether R-nylon fiber can be used as an additive to sprayed polymer cement mortar (SPCM) to improve the structural performance of SPCM repairs. In this study, a novel R-nylon fiber SPCM was compared with two common types of SPCM: polyethylene (PE) fiber SPCM, and plain SPCM (without fiber). The experiments involved the removal of concrete to three depths, to represent three repair methods: removal to a depth of 10 mm, removal of all the cover concrete, and removal to a depth of 20 mm over the tensile reinforcements. Four-point bending tests were conducted on 38 reinforced concrete (RC) beams whose flexural behaviors (load carrying capacity, flexural stiffness and ductility) were investigated. SPCM containing R-nylon fiber was found to afford increases in load carrying capacity for the beams whose tensile reinforcement was reduced by 10% to 18% from corrosion, and it was found to provide higher ductility than the two common types of SPCM. The beams repaired with SPCM containing either of the fibers showed higher stiffness than those repaired with SPCM without fibers. It was found that, for the beams whose tensile reinforcement was reduced by 10% from corrosion, removing the whole concrete covering is suitable for improving flexural behavior and can be a better choice in terms of economic efficiency. Furthermore, for beams that have lost 10% to 18% of their tensile steel mass, it is recommended that concrete over the tensile reinforcements be removed to a depth of 20 mm and replaced by SPCM containing either type of fibers.

Acknowledgement

It has been three years of learning for me, not only in the academic area, but also on a personal level. Today is the day: writing this note of thanks is the finishing touch on my dissertation. I would like to reflect on the people who have supported and helped me throughout these years.

My heartfelt gratitude goes first to my supervisor Pro. Hiroshi YOKOTA, for the continuous support of my Ph.D study and related research for his patience, kind supervision, and valuable guidance. His support and encouragement made it possible to achieve the goal. I could not have imagined having a better advisor and mentor for my Ph.D study.

Besides my supervisor, I am sincerely grateful to all esteemed members of the doctoral committee, Prof. Tamon UEDA and Prof. Takafumi SUKIYAMA for their comments and the hard question which incented me to widen my research from various perspectives.

My appreciation also extends to my lab mates in Lifetime Engineering Laboratory for their kind help and support contributes in many ways for conducting my experiments. In addition, I would like to thank my lab partner, Daiki UNNO, he supported me greatly and were always will to help me.

I gratefully acknowledge the material support provided by Sumitomo Osaka Cement (SOC) Co., Ltd., Japan. Dr. Makoto Yamamoto and staffs of SOC, are sincerely acknowledge for helping me to conduct some part of this experiment.

Last but not least, I would also like to thank my family for their wise counsel and sympathetic ear. You are always there for me. Finally, there are my friends. We were not only able to support each other by deliberating over our problems and findings, but also happily by talking about things other than just our researches.

List of Publications and Award

International Journals

1. Orasutthikul, S., Unno, D., Yokota, H. and Hashimoto, K. Effectiveness of recycled nylon fiber as a reinforcing material in mortar. Journal of Asian Concrete Federation, 2 (2), 102-109, 2016. (DOI: 10.18702/acf.2016.12.2.2.102)
2. Orasutthikul, S., Unno, D. and Yokota, H. Effectiveness of recycled nylon fiber from waste fishing net with respect to fiber reinforced mortar. Construction and Building Materials, 146, 594-602, 2017. (DOI: 10.1016/j.conbuildmat.2017.04.134)

International Conferences

1. 海野太貴，横田弘，橋本勝文，Orasutthikul, S. リサイクルナイロン繊維のモルタル補強材 としての有効性，平成 27 年度土木学会北海道支部論文報告集，72，札幌，2016 年 1 月 30- 31 日
2. Orasutthikul, S., Yokota, H., Hashimoto, K. and Unno, D. Effect of recycled nylon fiber on mechanical properties of mortar, 平成 27 年度土木学会北海道支部論文報告集，72，2016 年 1 月 30-31 日
3. Orasutthikul, S., Yokota, H., Hashimoto, K. and Unno, D. Effectiveness of recycled nylon fibers as a mortar strengthening material, Proceedings of International Symposium on Concrete and Structures for Next Generation (Ikeda & Otsuki Symposium), Tokyo, Japan, 16-18 May 2016, 241- 250.
4. 海野太貴，Orasutthikul, S.，横田 弘，橋本勝文．漁網を利用したリサイクルナイロン繊維 のモルタル補強材としての有効性，コンクリート工学年次論文集，38 (1)，1857-1862，2016.
5. Orasutthikul, S., Yokota, H., Hashimoto, K. and Unno, D. Effectiveness of recycled nylon fibers in mortar comparing with recycled PET and PVA fibers, Proceedings of 4th International Conference on Sustainable Construction Materials and Technologies (SCMT4), Las Vegas, USA, 7-11 August 2016, 1691-1700.
6. Orasutthikul, S., Yokota, H., Hashimoto, K. and Unno, D. Effectiveness of recycled nylon fiber as a reinforcing material in mortar, Proceeding of the 11th fib International PhD Symposium in Civil Engineering, Tokyo, Japan, 29-31 August 2016, 85-92.
7. 海野太貴，横田弘，Orasutthikul, S.，上松瀬慈．混入条件の違いによるリサイクルナイロン 繊維のモルタル補強効果に関する検討，土木学会第 71 回年次学術講演会講演概要集，V- 256，仙台，2016 年 9 月 7-9 日，511-512.
8. Orasutthikul, S., Unno, D., Yokota, H., and Hashimoto, K. Effectiveness of recycled nylon fiber as a reinforcing material in mortar, Proceedings of the 7th International Conference of Asian Concrete Federation (ACF 2016), Hanoi, Vietnam, 30 October-2 November, 2016.
9. Orasutthikul, S., Unno, D. and Yokota, H. Applicability of recycled-nylon fiber polymer cement mortar to the section repair of deteriorated RC beams, Proceedings of the 8th Asia and Pacific Young Researchers and Graduates Symposium (YRGS), Tokyo, Japan, 7-8 September 2017 (Accepted).
10. Orasutthikul, S., Unno, D. and Yokota, H. Structural performance evaluation of corrosion damaged RC beams repaired using sprayed polymer cement mortar with recycled nylon fiber, Proceedings of the 2nd ACF Symposium, Chiang Mai, Thailand, 23-25 November

2017 (Accepted).

Award

1. IOS Young Award 2016, International Symposium on Concrete and Structures for Next Generation, “Effectiveness of recycled nylon fibers as a mortar strengthening material.”

Table of Contents

List of Figures

List of Tables

CHAPTER 1

INTRODUCTION

1.1 PROBLEMS

Marine debris is one of the major problems in the sea and ocean environment. It has been reported that more than half of the debris that were dumped or lost directly into the seas, about 640,000 tons, are fishing nets (Figure 1.1). Almost 700 marine species including marine mammals are at risk; in particular, large whales, seals, and sea lions have been found entangled in the fishing nets (Figure 1.2 and 1.3). These abandoned fishing nets and debris also disturb marine ecosystem. They block sunlight to reach smallest creatures in the sea, which directly affects marine animals that feed on smallest creatures such as algae and plankton, as shown in Figure 1.4. Nowadays, fishing nets are mostly made of nylon which is non-biodegradable, and totally entangled fishing nets are very difficult to be separated. Therefore, there have been strong calls for recycling waste fishing nets.

Figure 1.1: Each year an estimated 640,000 tons of fishing net is abandoned in oceans, seas and bays [1, 2].

Figure 1.2: Fishing nets continue to catch marine lives even they have been abandoned [3]

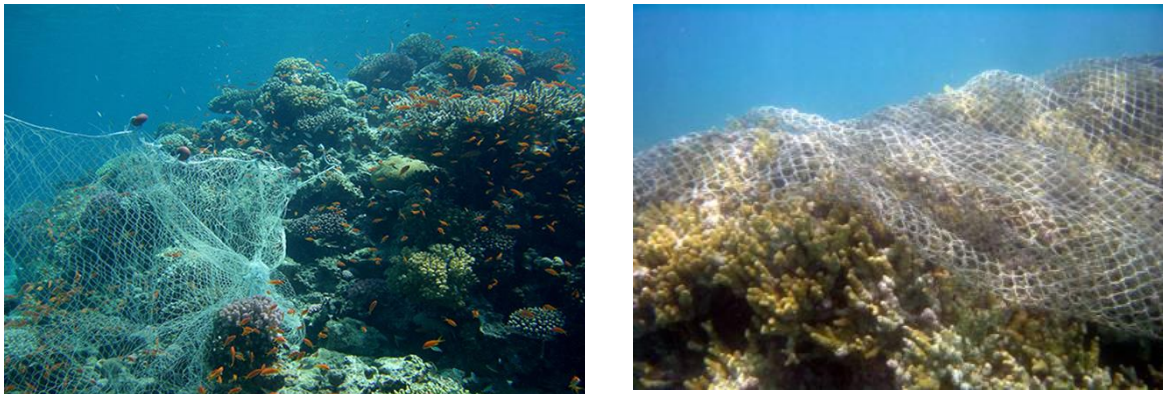

Figure 1.3: Corals can be damaged by abandoned fishing nets [4, 5].

Figure 1.4: Plastic garbage and waste fishing nets collect together on the surface of the ocean blocking sunlight to small creatures below them.

To meet such demands, a practical, suitable way to recycle them has been sought by many companies, while using recycled and renewable materials have been paid more attention [6]. The waste fishing nets are used in manufactures of carpet tiles, as well as they are melted and then used in manufactures of bicycle seats, chair and luggage castors, tool handles, electronics components, and other goods [7]. The nets have been also used in civil engineering field as a recycled fiber in order to reinforce or strengthen concrete, mortar and soil [8, 9]. Even during the past three decades, the use of synthetic fiber, such as polyvinyl alcohol (PVA) fiber and polypropylene fiber has been paid attention, and it is successful in significantly improving mechanical properties, such as flexural strength, fracture toughness, and impact resistance, of fiber reinforced mortar and concrete [10-25]. However, using of those fibers surely leads to higher energy consumption and emission for production process [9]. Accordingly, many researchers have been concerning and focusing on using recycled materials [24, 26-32], in recent years. Kim et al. [8] studied the mechanical properties of reinforced lightweight soil (RLS) by using waste fishing nets. They found that using waste fishing nets at 0.25% by weight of soil makes unconfined compressive strength of RLS 2-2.5 times higher than that of untreated lightweight soil. Spadea et al. [9] investigated the static mechanical properties of fiber reinforced mortar by using recycled nylon fiber from abandoned fishing nets. They found that

the toughness and ductility are significantly improved by the addition of recycled fiber to the mortar, and the flexural strength is improved up to 35%. Alkali degradation of the nylon fiber may occur if it is mixed with cement, which results in reduction in strength and toughness of the fiber reinforced concrete. Ochi et al. [33] investigated the alkali resistance of synthetic fibers such as PET, polypropylene and PVA fibers by doing immersion tests into alkali solution. They found that tensile strength of PET, polypropylene and PVA fibers decrease 99%, 86% and 56% of respective virgin fibers. For the recycled nylon fiber, Spadea et al. [9] found that its tensile strength decreases only about 4% by the exposure to an alkali environment. The author previously conducted a comparative experimental research on the effectiveness of recycled nylon fiber and PVA fiber reinforced mortar [34]. The research concluded that recycled nylon fiber has a potential to improve the mechanical properties of mortar.

1.2 THEORETICAL BACKGROUND

1.2.1 Toughness and residual strength

ASTM C1018 [35] standard test method evaluates the flexural performance of fiber-reinforced concrete by testing a simply supported beam under third-point loading. From this test, toughness indices can be derived in terms of the area under a load-deflection curve.
The behavior of the fiber-reinforced mortar up to the load at which first crack occurs can be defined by the first-crack strength. The behavior thereafter, is defined by the toughness indices, which also reflect the post peak behavior.
The first-crack strength can be calculated using the equation presented in the ASTM C293 "Standard test method for flexural strength of concrete" [36] as follows:

$$f_b = 3P_{cr}l/2bd^2$$

Where:
f_b = first crack strength
P_{cr} = maximum applied load indicated by the testing machine
b = specimen width
d = specimen depth
l = span length

As shown in Figure 1.5, the first crack deflection, δ, is characterized by the distance from O to H. Toughness indices I_5, I_{10} and I_{20} are obtained by dividing the area under the load-deflection curve up to 3.0, 5.5, and 10.5 times the first-crack deflection, respectively, by the area under the curve up to the first-crack deflection.
The toughness indices are calculated as follows:

$$I_5 = \text{Area } OABG / \text{Area } OAH$$
$$I_{10} = \text{Area } OACF / \text{Area } OAH$$
$$I_{20} = \text{Area } OADE / \text{Area } OAH$$

Where:
I_5 = Toughness index up to 3.0 times the first crack deflection
I_{10} = Toughness index up to 5.5 times the first crack deflection
I_{20} = Toughness index up to 10.5 times the first crack deflection

The residual strength factors, $R_{5,10}$ and $R_{10,20}$, were determined according to ASTM C1018 by the following equations:

$$R_{5,10} = \frac{100}{(5-10)}(I_5 - I_{10}) \quad (1)$$

$$R_{10,20} = \frac{100}{(10-20)}(I_{10} - I_{20}) \quad (2)$$

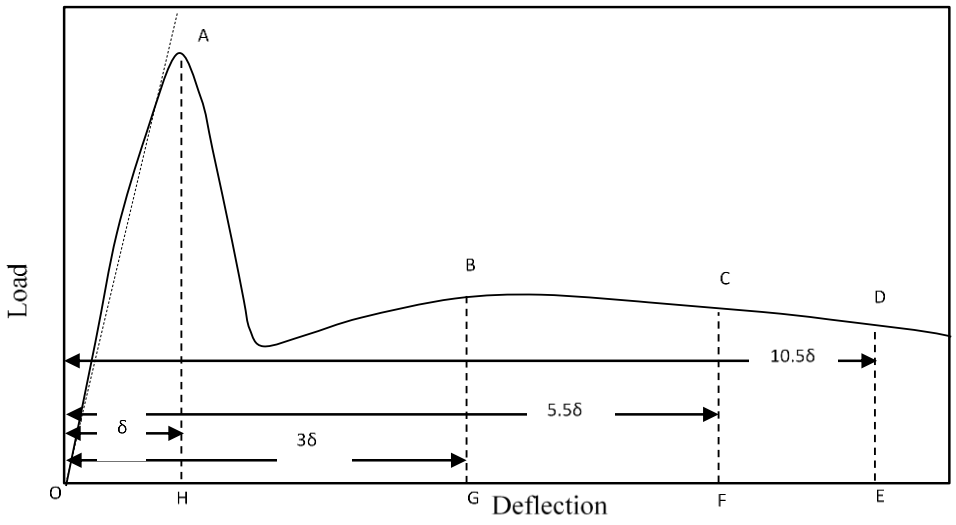

Figure 1.5: Toughness indices as defined by ASTM 1018 [35].

1.2.2 Ductility

The ductility of reinforced concrete (RC) structures is an important properties, it is considered as the ability to ensure the structure subjected to critical load sustain inelastic deformation without considerable degradation of load carrying capacity, prior to ultimate collapse. Significant loss of ductility has been reported in the context of repaired and strengthened RC beams using several techniques. Thomsen et al. [2004] suggested two definitions of ductility, one displacement-based, the other energy-based, which are illustrated in Figure 1.6, and are then defined as

Energy ductility: $$D_E = \frac{E_u}{E_y} \quad (1)$$

Deflection ductility: $$D_D = \frac{\Delta_u}{\Delta_y} \quad (2)$$

Where E_y and E_u can be calculated as the area under the load deflection curve up to yield and ultimate respectively, and Δ_y, Δ_u represent the deflection at yield and ultimate respectively.

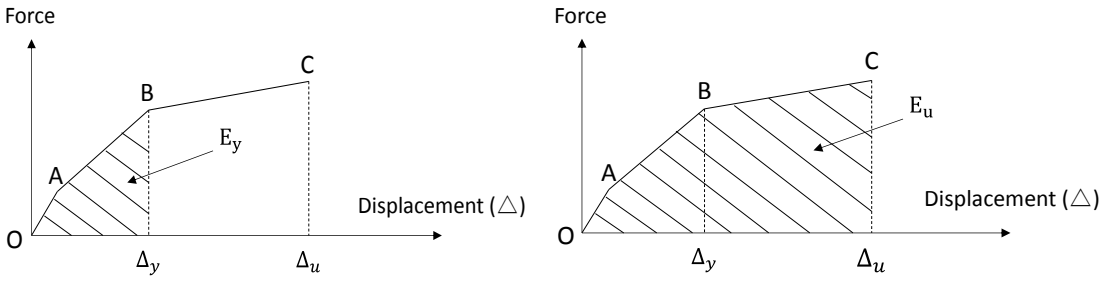

Figure 1.6: Definition of energy ductility used by Thomsen et al 2004 [37]

1.2.3 Steel corrosion

Steel reinforcement inside the concrete is generally protected from rusting by high alkalinity of the concrete. This is because in the high alkalinity environment, steel is passive to the anodic reaction. It means that steel will not dissolve into ion of the steel (Fe^{2+}) and electron ($2e^-$). The normal ranges of pH in the concrete are from 12.5 to 13.5, depending on mix proportion and the mixing materials especially the cementitious materials. This condition is usually referred to as passivity of the steel bars in the concrete. Passivity of the steel bars in the concrete is sometime described by the development of thin films of oxide of the steel that prohibits anodic reaction to further develop. Quality of the concrete covering the steel reinforcement is another important factor that control the corrosion behavior of the steel bars in the concrete since the electrochemical reaction of corrosion requires electrolyte that is in this case the pore water in the concrete. Quality of the concrete cover also controls the diffusivity of detrimental ions and gases into the concrete.

1.2.3.1 Mechanisms

Corrosion of the reinforcing bars in concrete can occur when the following conditions are achieved.

a) Depassivation of the steels. The passivity of the steel bars in the concrete can be destroyed in two ways as follows.

- Alkalinity of the concrete surrounding the steel bars is reduced to a critical values may range from 9 to 10.5 depending on many factors such as mix proportion and type of binder. The reduction of alkalinity in the concrete can be caused by many processes such as carbonation and leaching, etc. When concrete has high porosity and is subjected to hydraulic pressure, the movement of water through the pores in concrete can reduce the alkalinity of the concrete. Penetration of chloride ion into the concrete also plays some parts in the alkalinity reduction of the concrete due to ion exchange behavior, however, in case of chloride induced steel corrosion, the critical chloride content is the main factor to decide the corrosion initiation.
- Chloride content especially free chloride content around the steel bars arrives at its critical chloride content. The critical chloride content also depends on various factors. A popular

method to estimate the critical chloride content is to use the ratio between the chloride ion and the hydroxyl ion in the pore solution of the concrete as an index.

Anodic reaction, which involves the dissolving of the steel into ion of the steel and electrons, can be initiated when the passivity of the reinforcement is destroyed.
b) There is enough moisture. The ion of the steel (Fe^{2+}) must be dissolved in the pore solution which needs water. The formation of rust also requires water. Normally, concrete surrounding steel bars contains enough water content for the reaction.
c) There is enough supply of oxygen for the corrosion process. Oxygen is usually supplied into the concrete through the unsaturated pores. Pore water blocks the transport of oxygen into the concrete through the water-saturated pores. In saturated concrete, oxygen may dissolve and move into the concrete through the water saturated pores but the solubility of the oxygen in water is usually considered negligible for this problem. Consequently, corrosion of the reinforcing steels is seldom observed in reinforced concrete structures that are always submerged in water or saturated.

Figure 1.7 illustrates the process of steel corrosion in the concrete. The process of steel corrosion starts from the depassivation of the steel bars which may be caused by one or more of the aforementioned reasons. Also moisture around the steel bars must be enough for promoting the electrochemical reactions that lead to corrosion. Then the process starts from dissolution of the steel into ion (Fe^{2+}) and electron ($2e^-$) as in Eq. (1.1). The ion, Fe^{2+}, dissolves into the pore solution of the concrete and the electron, $2e^-$, travel mostly through the steel bars. This reaction is called anodic reaction with the process named similarly as "anodic process".

$$Fe \longrightarrow Fe^{2+} + 2e^- \qquad (1.1)$$

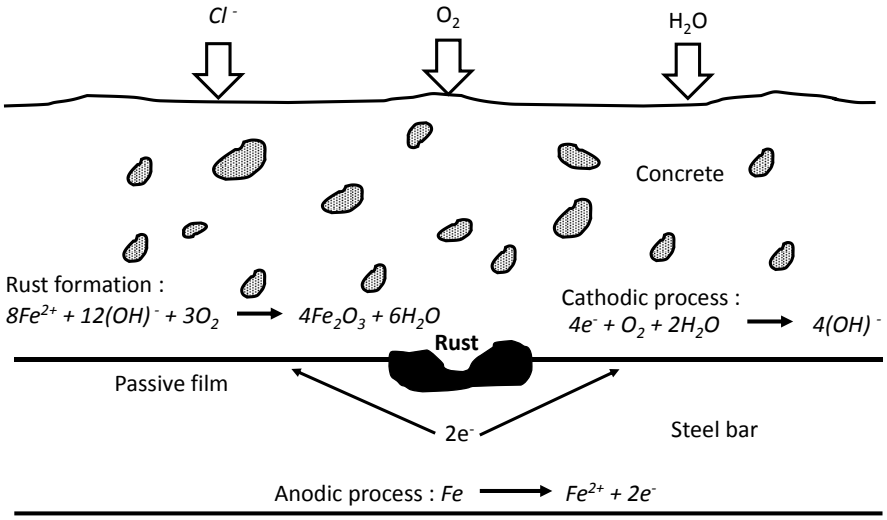

Figure 1.7: Mechanisms of steel corrosion in concrete

As generally known, anodic process is the process that a metal loses its electron. The released electrons then combine with water and oxygen at some locations which can even be somewhere remote from the location where anodic process occurs. The action produces hydroxyl ion as follows.

$$4\,e^- + O_2 + 2H_2O \longrightarrow 4(OH)^- \qquad (1.2)$$

This process is called "cathodic process". Again, one may know that cathodic process involves the receiving of electron. After that rust will be formed by the following reaction.

$$8\,Fe^{2+} + 12(OH)^- + 3\,O_2 \longrightarrow 4Fe_2O_3 + 6\,H_2O \qquad (1.3)$$

The Fe_2O_3 is ferric oxide or rust. The reaction shown in Eq. (1.3) can occur in any location, on the surface of the steel bars, which is sometimes different from the places where anodic or cathodic processes occur. In other words, rust is not necessary formed only at the location where the corroding steel bar loses its cross section.

1.2.3.2 Effect of Corrosion on Reinforced Concrete Structures

There are two main causes that make reinforced concrete structures lose their load carrying capacity are as follows.

1) The corroded steel bars lose a part of their cross section at the location where anodic reaction had been processed. This happens because a part of the steel dissolved into the pore solution of the concrete and become Fe^{2+} and $2e^-$ as explained. The localized reduction of the steel bar reduces its load carrying and results in the reduction of the performance of the overall reinforced concrete member where the corroded steel is contained. Load carrying capacity, stiffness and ductility of reinforced concrete member will be reduced with the increase in member deflection. The fatigue strength of the member decreases dramatically due to the localized stress at the reduced cross section of the bar.

2) Rust formed on the surface of the steel bars exerts large pressure on the concrete cover due to its larger volume comparing with the original steel that had been dissolved in the anodic reaction. In many cases, the volume of the rust may be as large as 6 to 10 times of the original steel especially when there is plenty supply of water and oxygen. This pressure can lead to splitting cracks in the concrete cover along the alignment of steel bars. This splitting cracks will accelerate the rate of corrosion since chloride, carbon dioxide, moisture and oxygen can easily diffuse into the concrete through the cracks. The splitting cracks reduces bond strength between concrete and steel bars and are dangerous to the ductility, fatigue strength and load carrying capacity of the reinforced concrete members.

1.3 RESEARCH OBJECTIVES

This research investigates in detail the effectiveness of recycled (R-) nylon fiber from waste fishing nets when they are mixed into mortar. The mechanical properties such as compressive strength, flexural strength, toughness and residual strength were analyzed and compare with those of mortar with recycled polyethylene terephthalate (PET) and polyvinyl alcohol (PVA) fibers that have been frequently used as reinforcing materials of mortar and concrete. In the

first stage of this research, the objectives are as follows:
1. To analyze the effectiveness of using waste fishing nets as R-nylon fiber to reinforce mortar.
2. The fiber length and fiber volume fraction are focused to analyze the mechanical properties including compressive strength, flexural strength, toughness and residual strength as well as flowability of each fresh mix.
3. To compare the effectiveness of R-nylon fiber on reinforcing mortar with two common types of fiber that are recycled PET and PVA fibers.

After investigation of possibility to use R-nylon fiber from waste fishing nets, the author discusses whether R-nylon short fiber can be used as an additive to sprayed polymer cement mortar (SPCM) to improve the structural performance of corrosion damaged RC beam. This study has following main aims and objectives:
1. To investigate structural behavior and performance of the repaired beams in terms of load carrying capacity, flexural stiffness and ductility as well as crack formation with bending tests that focused on the following test parameters: repair method, SPCM type and level of corrosion damage.
2. To compare repair effectiveness of the R-nylon fiber SPCM with two common SPCM types, which are polyethylene (PE) fiber SPCM, and plain SPCM (without fiber).
3. This study is expected to contribute to guidelines for SPCM repairs to corrosion-damaged RC beams.

1.4 THESIS STRUCTURE

This thesis is divided into five chapters as explained below:

Chapter one gives problems of abandoned fishing nets and possible way to recycle them, and a brief theory background to mechanical properties of fiber reinforced mortar, ductility of RC beam, and steel corrosion mechanism along with the objectives of the present study and thesis layout.

In chapter two, investigation of using R-nylon fiber as reinforcing material in mortar is described. The mechanical properties of R-nylon fiber reinforced mortar (FRM) including flexural strength, compressive strength, toughness and residual strength as well as flow ability were discussed in comparison with virgin fiber that is PVA fiber and recycled PET fiber which are commonly used.

Chapter three provides the effect of R-nylon fiber polymer cement mortar which focusing on spraying method on the rehabilitation of corrosion damage RC beam. A novel R-nylon fiber SPCM was compared with two common types of SPCM: PE fiber SPCM and plain SPCM (without fiber). Four-point bending tests were conducted on a series of corrosion-damaged RC beams repaired with SPCM. Flexural behavior was investigated in terms of load carrying capacity, flexural stiffness and ductility as well as crack formation with bending tests that focused on the following test parameters: repair method, SPCM type and level of flexural reinforcement corrosion.

Chapter four, comparison of structural behavior and performance of repaired corroded RC beams with different repair plan at a given corrosion level was done. The structural

performance such as load carrying capacity and ductility as well as crack formation was analyzed.

The fifth chapter gives conclusions and some recommendations for future work.

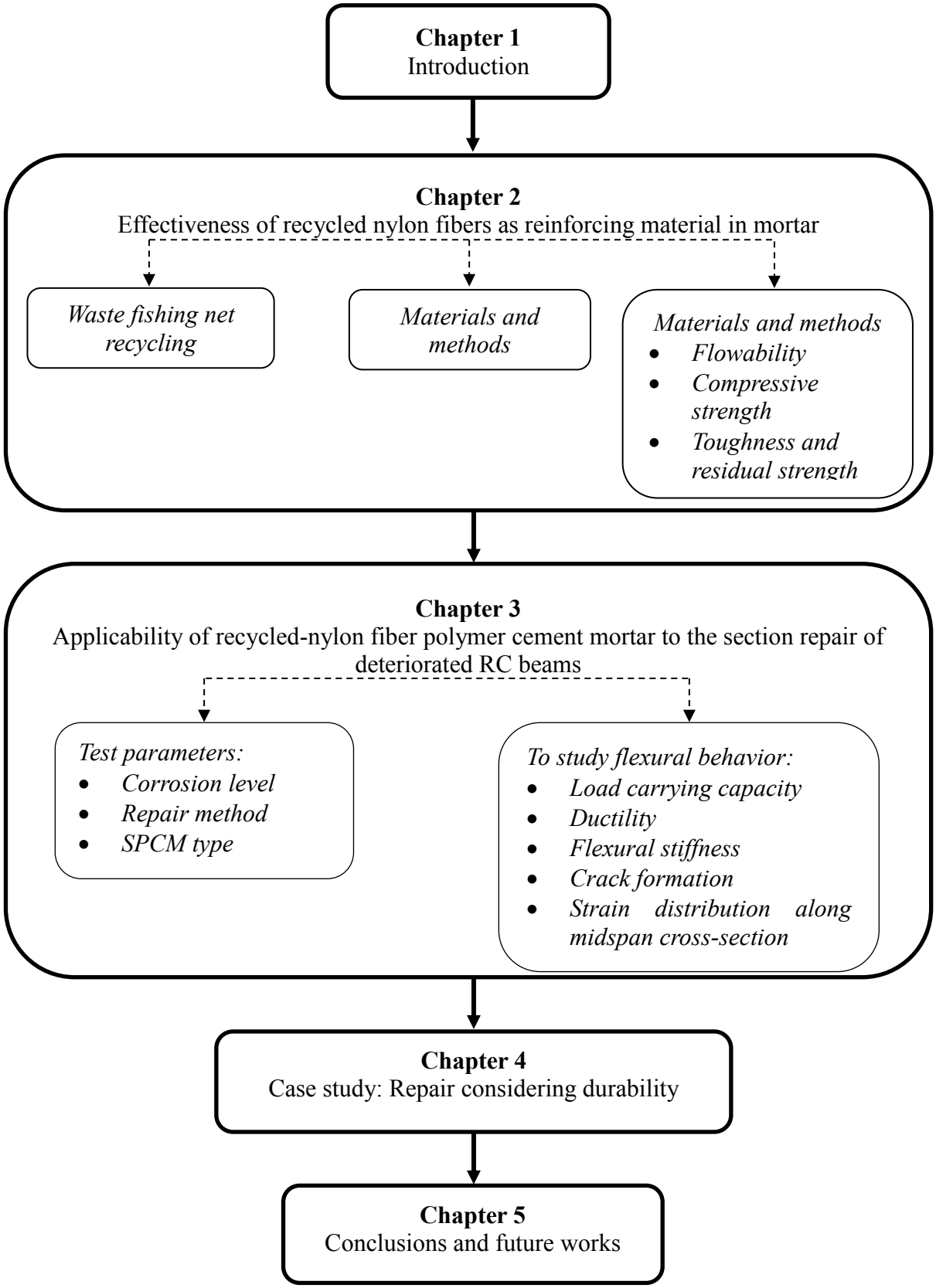

Figure 1.8: Outline of Thesis Chapters

1.3 REFERENCES

1. Sea Around Us. <http://www.seaaroundus.org> (Accessed on April 4, 2016).
2. Ocean Outcomes. <http://www.oceanoutcomes.org> (Accessed on April 7, 2017).
3. Ocean Health Index. < http://www.oceanhealthindex.org> (Accessed on October 29, 2014).
4. Earth Island Journal. <http://earthisland.org> (Accessed on January 7, 2014)
5. NOAA's Marine Debris Blog. <https://marinedebrisblog.wordpress.com> (Accessed on December 1, 2016)
6. TriplePundit. <http://www.triplepundit.com> (Accessed on November 14, 2016)
7. Coastal Plastic Recycling. <http://www.coplare.net>
8. Kim Y. T., Kim, H. L. and Lee G. H. (2008). "Mechanical behavior of light soil reinforced with waste fishing net." *Geotextiles and Geomembranes,* 26, 512-518.
9. Spadea, S., Farina, I., Carrafiello, A. and Fraternali, F. (2015). "Recycled nylon fibers as cement mortar reinforcement." *Construction and Building Materials*, 80, 200-209.
10. Hughes, B. P. and Fattuhi N. I. (1976). "Improving the toughness of high strength cement paste with fibre." *Composites*, 7(4), 185-188.
11. Mindess, S., Banthia, N. and Benthur, A. (1986). "The response of reinforced concrete beams with a fibre concrete matrix to impact loading." *International Journal of Cement Composite and Light-Weight Concrete*, 8(3), 165-170.
12. Mindess, S. and Vondran, G. (1988). "Properties of concrete reinforced with fibrillated polypropylene fibers under impact loading." *Cement and Concrete Research*, 18, 109-115.
13. Wang, Y., Li, V. C. and Backer, S. (1990). "Tensile properties of synthetic fiber reinforced mortar." *Cement and Concrete Composites*, 12(1), 29-40.
14. Alhozaimy, A. M., Soroushian, P. and Mirza, F. (1996). "Mechanical properties of polypropylene fiber reinforced concrete and the effects of pozzolanic materials." *Cement and Concrete Composites*, 18(2), 85-92.
15. Song, P. S., Hwang, S. and Sheu, B. C. (2005). "Strength properties of nylon and polypropylene-fiber-reinforced concretes." *Cement and Concrete Research*, 35(8), 1546-1550.
16. Ozerkan, N. G., Ahsan, B., Mansour, S. and Iyengar, S. R. (2013). "Mechanical performance and durability of treated palm fiber reinforced mortars." *International Journal of Sustainable Building Environment*, 2(2), 131-142.
17. Banthia, N., Zanotti, C. and Sappakittikorn, M. (2014). "Sustainable fiber reinforced concrete for repair applications." *Construction and Building Materials*, 67 (Part C), 405-412.
18. Jang, J. G., Kim, H. K., Kim, T. S., Min, B. J. and Lee, H. K. (2014). "Improved flexural fatigue resistance of PVA fiber-reinforced concrete subjected to freezing and thawing cycles." *Construction and Building Materials*, 59, 129-135.
19. Kwon, M. H., Jung, W. Y. and Seo, H. S. (2014). "The flexural strength of fiber reinforced polymer cement mortars with using UM resin." *International Journal of Civil, Environmental, Structural, Construction and Architectural Engineering*, 8(2), 127-130.
20. Erdogmus, E. (2015). "Use of fiber reinforced cements in masonry construction and structural rehabilitation." *Fibers*, 3, 41-63 (doi:10.3390/fib3010041).
21. El-Gamal, S. E., Al-Nuaimi, A., Al-Saidy, A. and Al-Lawati, A. (2016). "Efficiency of near surface mounted technique using fiber reinforced polymers for the flexural strengthening of RC beams." *Construction and Building Materials*, 118, 52-62.

22. Khan, U. S. and Ayub, T. (2016). "Modelling of the pre and post-cracking response of the PVA fibre reinforced concrete subjected to direct tension." *Construction and Building Materials*, 120, 540-557.
23. Mohseni, E., Khotbehsara, M. M., Naseri, F., Monazami, M. and Sarker, P. (2016). "Polypropylene fiber reinforced cement mortars containing rice husk ash and nano-alumina." *Construction and Building Material*, 111, 429-439.
24. Yin, W., Tuladhar, R., Riella, J., Chung, D., Collister, T. and Combe, M. (2016). "Comparative evaluation of virgin and recycled polypropylene fibre reinforced concrete." *Construction and Building Materials*, 114, 134-141.
25. Nuruddin, M. F., Khan, S. U., Shafiq, N. and Ayub, T. (2014). "Strength development of high strength ductile concrete incorporating Metakaolin and PVA fibers." *The Scientific World Journal*, 2014, Article #387259, 1-11.
26. Silva, D. A., Betioli, A. M., Gleize, P. J. P., Roman, H. R., Gomez, L. A. and Ribeiro, J. L. D. (2005). "Degradation of recycled PET fibers in Portland cement-based materials." *Cement and Concrete Research*, 35(8), 1741-1746.
27. Foti, D. (2011). "Preliminary analysis of concrete reinforced with waste bottles PET fibers." *Construction and Building Materials*, 25, 1906-1915.
28. Pereira de Olivia, L. A. and Castro-Gomes, J. P. (2011). "Physical and mechanical behavior of recycled PET fibre reinforced mortar." *Construction and Building Materials*, 25, 1712-1717.
29. Fraternali, F., Farina, I., Polzone, C., Pagliuca, E. and Feo, L. (2013). "On the use of R-PET strips for reinforcement of cement mortars." *Composites B*. 46, 207-210.
30. Habib, A., Begum, R. and Alam, M. M. (2013). "Mechanical properties of synthetic fibers reinforced mortars." *Internal Journal of Scientific and Engineering Research*, 4(4), 923-927.
31. Ozger, O. B., Girardi, F., Giannuzzi, G. M., Salomoni, V. A., Majorana, C. E., Fambri, L., Baldassino, N. and Maggio, R. D. (2013). "Effect of nylon fibers on mechanical and thermal properties of hardened concrete for energy storage systems." *Materials and Design*, 51, 989-997.
32. Pesic, N., Zivanovic, S., Garcia, R. and Papastergiou, P. (2016). "Mechanical properties of concrete reinforced with recycled HDPE plastic fibres." *Construction and Building Materials*, 115, 362-370.
33. Ochi, T., Okubo, S. and Fukui, K. (2007). "Development of recycled PET fiber and its application as concrete-reinforcing fiber." *Cement and Concrete Composites*, 29, 448-455.
34. Orasutthikul, S., Unno, D., Yokota, H. and Hashimoto, K. (2016). "Effectiveness of recycled nylon fiber as a reinforcing material in mortar." *Proceedings of the 7th International Conference of Asian Concrete Federation*, 30 Oct – 2 Nov, Hanoi, Vietnam.
35. ASTM C 1018. "Standard test method for flexural toughness and first-crack strength of fiber reinforced concrete," ASTM International, PA.
36. ASTM C 293. "Standard test method for flexural strength of concrete (Using simple beam with center point loading)," ASTM International, PA.
37. Thomsen, H., Spacone, E., Limkatanyu, S. and Camata, G. (2004). "Failure mode analyses of reinforced concrete beams strengthened in flexure with externally bonded fiber-reinforced polymers." *Journal of Composites for Construction*, ASCE, 8(2), 123-131.

CHAPTER 2

EFFECTIVENESS OF RECYCLED NYLON FIBERS AS REINFORCING MATERIAL IN MORTAR

2.1 OVERVIEW

This chapter discusses the utilization of recycle waste fishing nets in fiber reinforced mortar. Experimental test results compared the mechanical properties of such mortar made with recycled nylon fiber to those of such mortar made with recycled PET and PVA (polyvinyl alcohol) short fibers. The recycled nylon (R-Nylon) fibers were obtained by manually cutting of waste fishing nets to the lengths of 20 mm, 30 mm and 40 mm. Two types of R-Nylon fibers were investigated that are straight and knotted types. The addition of straight R-Nylon fiber improved the flexural strength up to 41% in comparison with that of the knotted R-Nylon, recycled PET, and PVA fibers. The compressive strength of the mortar with R-Nylon fiber decreased with increase in fiber fraction and length. The post peak load, toughness and residual strength depended on the properties of fiber such as Young's modulus, tensile strength, and geometry as well as the bond strength between fiber and matrix.

2.2 EXPERIMENTAL PROGRAM

2.2.1 MIXTURE COMPOSITION AND PREPARATION

The recycled nylon fiber examined in this study was prepared by manually cutting waste fishing nets collected by fishermen in Hokkaido, see Figure 2.1(a). The cutting was started after washing the net by tap water. The two fiber types were made; that is, straight fiber and knotted fiber, see Figures 2.1(b) and 2.1(c), respectively. The straight fiber was 20 mm, 30 mm or 40 mm long, and was mixed in mortar at the volume fractions of 1.0%, 1.5% and 2.0%. The knotted fiber was 40 mm long, and was mixed in mortar at the volume fractions of 0.5%, 0.75% and 1.0%. The volume fractions of the knotted fiber are less than those of the straight fiber because the knotted fiber tends to form tenacious balls easily. PVA and R-PET fibers were supplied by Kuraray Company and Sango Company, respectively. They were mixed in mortar at the volume fractions of 1.0% and 1.5%. In this study, the uniaxial tensile tests according to ASTM C1557-03 [1] were carried out to determine Young's modulus and tensile strength of recycled nylon fiber, as shown Figure 2.2. The appearances and properties of all the fibers are summarized in Figure 2.1 and Table 2.1, respectively.

Firstly, cement and sand were mixed by using small mixer, and after that, fibers were gently added to prevent the formation of fiber balls. To ensure uniform fiber dispersion, all dry components were mixed by hand. Then, water was gradually added to the mix, and the mixing was continued to blend all ingredients for other 2 minutes so that a homogeneous mixture and proper workability were achieved. The mass ratio of sand with cement of the mortar was 3.0 and the water-to-cement ratio was 0.5. All molds were covered with plastic sheet to minimize moisture evaporation for a period of 24 hours after placing. Subsequently, the specimens were cured in a water tank at 20±2 ˚C for 28 days. As presented in Table 2.2, the mortar mixes vary due to types, volume and the aspect ratio of fiber. The unreinforced mortar is denoted as UR,

and the fiber reinforced mortar specimens are noted as “KN”, “SN”, “PE” and “PV,” followed by “fiber length – volume fraction,” to represent recycled knotted nylon fiber, recycled straight nylon fiber, recycled PET fiber and PVA fiber, respectively.

(a) Waste fishing net

(b) Straight R-Nylon fiber

(c) Knotted R-Nylon fiber

(d) PVA fiber (18 mm)

(e) PVA fiber (30 mm)

(f) R-PET fiber

Figure 2.1: Types of fibers

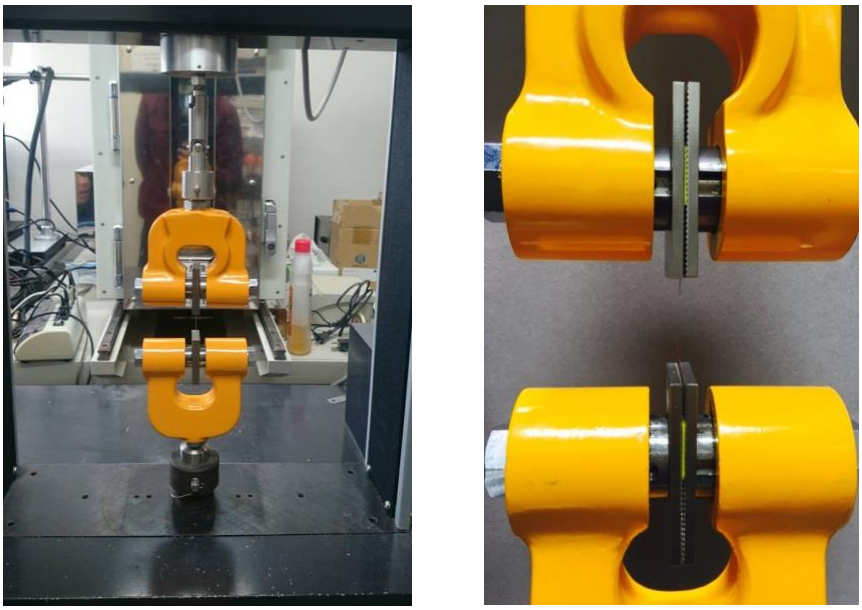

Figure 2.2: Uniaxial tensile test

Table 2.1: Properties of the fibers

Fiber type	Diameter (mm)	Tensile strength (MPa)	Young's modulus (GPa)	Density (g/cm^3)
R-Nylon	0.35	440	3.0	1.13
R-PET	0.70	450	20	1.32
PVA (18 mm)	0.20	975	27	1.30
PVA (30 mm)	0.66	900	23	1.30

2.2.2 TESTING METHODS

The mortar flow test was conducted in accordance with ASTM C 1437 [2]. Compressive strength was determined in compliance with ASTM C 39 [3]. Flexural strength tests were conducted in accordance with ASTM C 1018 [4]. The authors performed three-point bending tests, and measured the peak load, first crack strength, toughness indices and residual strength factors. Two Linear Variable Differential Transformer (LVDT) were used to measure deflection, and were installed each side of the specimen at midspan, as shown in Figure 2.3. For each mix design, the mortar was cast in cylinders of 50 mm diameter × 100 mm in height for the compressive test and in prism molds of 40 mm × 40 mm × 160 mm for the bending test. For each mix, three and two specimens were tested for compressive and flexural strengths, respectively, after curing for 28 days.

Figure 2.3: Three point bending test setup

Table 2.2: Specimen types and test results of mortar flow

Specimen type	Fiber fraction by volume (%)	Fiber length (*L*) (mm)	Fiber diameter (*D*) (mm)	Aspect ratio (*L/D*)	Mortar flow (mm)
UR	0	-	-	-	260
KN-40-0.5	0.5	40	0.35	114	247
KN-40-0.75	0.75	40	0.35	114	233
KN-40-1.0	1.0	40	0.35	114	227
SN-20-1.0	1.0	20	0.35	57	231
SN-20-1.5	1.5	20	0.35	57	226
SN-20-2.0	2.0	20	0.35	57	207
SN-30-1.0	1.0	30	0.35	86	229
SN-30-1.5	1.5	30	0.35	86	216
SN-30-2.0	2.0	30	0.35	86	195
SN-40-1.0	1.0	40	0.35	114	217
SN-40-1.5	1.5	40	0.35	114	207
SN-40-2.0	2.0	40	0.35	114	183
PE-30-1.0	1.0	30	0.70	43	244
PE-30-1.5	1.5	30	0.70	43	219
PE-40-1.0	1.0	40	0.70	57	229
PE-40-1.5	1.5	40	0.70	57	196
PV-18-1.0	1.0	18	0.20	90	213
PV-18-1.5	1.5	18	0.20	90	169
PV-30-1.0	1.0	30	0.66	45	213
PV-30-1.5	1.5	30	0.66	45	189

2.3 RESULTS AND DISCUSSION

2.3.1 FLOWABILITY

The flow diameters were measured and are listed in Table 2.2 It can be seen that the flow diameter tends to decrease with increase in fiber length and amount. Moreover, if comparing 1% volume fraction of straight and knotted R-nylon fiber, the fresh mortar with knotted fiber has larger flow diameters. According to balling of KN fiber, which resulted in fiber-mortar separation, the mortar easily flows. For PET and PVA fibers, mortar flows exhibited the same results; that is, when the aspect ratio and fiber fraction increase, the flow diameter decreases. Furthermore, if comparing R-Nylon, PET and PVA fibers at the similar aspect ratio and the same fiber fraction, addition of R-Nylon, PET and PVA fibers into mortar results in more reduction in mortar flowability.

2.3.2 COMPRESSIVE STRENGTH

The compressive strengths of the fiber reinforced mortar at 28 days are presented in Table 3. The results indicate that the compressive strength decreases as the length decreases and as the amount of R-Nylon fibers increases. This can be explained that Young's modulus of mortar was reduced with the dosage of fibers with low Young's modulus, especially R-Nylon fibers [5, 6]. The Young's modulus of R-Nylon fiber is very low compared with that of mortar; therefore, inclusion of the fiber creates voids in mortar [7]. This might suggest that the lower compressive strength of the KN mortar is the result of a greater reduction in Young's modulus of the fiber reinforced mortar from the inclusion of knots, see Table 3. Additionally, poor fiber distribution according to easy forming ball of KN fiber, this results in reduction in compressive strength of KN mortar. Palmquist et al. [8] found that the addition of fiber, especially long fiber, leads to increase in the volume of interfacial transition zone which results in reduction of strength and stiffness of fiber reinforced mortar. Li [9] also investigated the effect of fiber addition on compressive strength of cementitious composites. In this work, it can be explained that a decrease of compressive strength is a result of low resistance to sliding of crack faces which is exerted by bridging force of fiber. Furthermore, when the specimens are subjected to compressive load, it induces lateral tensile strain in mortar due to the Poisson effect. As the load increases, longer fibers play an important role in mortar's lateral tensile strength than shorter ones. Therefore, the mortar postpone crack enlargement by increasing their lateral tensile strength [10]. This is the reason why the addition of shorter fiber provides lower compressive strength. Spadea et al. [11] also found that compressive strength of mortar with R-Nylon fiber decreased with increase in fiber fraction and decrease in fiber length. For R-PET and PVA fibers, the addition of these fibers into mortar reduces the mortar compressive strength. The moduli of elasticity of PVA and PET fibers are close to mortar; however, these fibers have low density. Therefore, mortar is mixed with large amount of fibers which results in reduction in its Young's modulus [6]. According to the addition of R-Nylon fiber into mortar, the specimens experienced softening behavior after the peak stress under compression test. On the other hand, plain mortar showed brittle tensile split failure by the formation of the crack parallel to the direction of applied load, as shown in Figure 2.4.

Table 2.3: Results of compressive strength and flexural strength tests

Specimen type	Compressive strength test				Flexural strength test			
	f'_c (MPa)	SD (MPa)	CV (%)	$\Delta f'_c$ (%)	f_b (MPa)	SD (MPa)	CV (%)	Δf_b (%)
UR	65.7	1.5	2.3	-	4.8	0.1	3.4	-
KN-40-0.5	56.6	6.9	12.1	-13.8	5.9	0.1	5.7	22.0
KN-40-0.75	56.0	11.4	20.4	-14.9	5.0	0.1	3.3	4.9
KN-40-1.0	36.8	6.0	16.2	-44.0	4.5	0.0	0.0	-7.4
SN-20-1.0	52.6	1.2	2.2	-20.0	6.1	0.1	5.5	26.8
SN-20-1.5	48.7	2.1	4.2	-25.9	6.8	0.2	9.7	41.4
SN-20-2.0	34.1	1.7	5.0	-48.0	4.8	0.1	3.4	-0.1
SN-30-1.0	53.6	0.6	1.1	-18.4	5.7	0.2	8.7	19.4
SN-30-1.5	46.8	1.0	2.2	-28.7	5.6	0.1	5.9	17.1
SN-30-2.0	35.1	3.3	9.5	-46.6	4.3	0.2	11.5	-9.8
SN-40-1.0	55.5	2.8	5.1	-15.4	6.0	0.2	8.3	24.4
SN-40-1.5	48.2	0.6	1.2	-26.5	6.4	0.1	2.5	34.0
SN-40-2.0	35.3	1.1	3.0	-46.3	5.2	0.1	6.4	7.3
PE-30-1.0	65.2	0.4	0.6	-0.5	4.9	0.0	0.0	2.4
PE-30-1.5	60.2	5.0	8.4	-8.2	5.2	0.4	19.2	7.3
PE-40-1.0	66.2	0.7	1.1	1.0	5.3	0.1	3.2	9.7
PE-40-1.5	60.8	5.1	8.4	-7.2	5.9	0.4	17.0	21.9
PV-18-1.0	62.9	1.9	2.9	-4.0	5.7	0.1	2.9	19.5
PV-18-1.5	62.5	0.9	1.4	-4.6	5.9	0.1	5.7	22.0
PV-30-1.0	62.2	2.1	3.3	-5.1	5.6	0.5	23.6	17.1
PV-30-1.5	61.1	2.9	4.8	-6.8	6.3	0.0	0.0	31.7

Note) f'_c is compressive strength; f_b is flexural strength; SD is standard deviation; CV is the coefficient of variation; and $\Delta f'_c$ and Δf_b are the percent difference in compressive strength and in flexural strength in comparison with respective control specimens (UR).

(a) Plain mortar (b) R-nylon fiber reinforced mortar

Figure 2.4: Failure modes of non-reinforced and reinforced mortar by compressive test

2.3.3 FLEXURAL STRENGTH

The flexural strengths are listed in Table 2.3. It is evident that the addition of R-Nylon fiber improves the flexural strength up to 41%, and it can be found that the optimum SN fiber fraction is 1.5% for improving the flexural strength. Spadea et al. [11] found that R-Nylon fiber is very effective in increasing flexural strength (up to 35%), especially when the longer fiber is used. KN, PE-30, PE-40, PV-18 and PV-30 fibers improved the flexural strength by up to 22%, 7%, 22%, 22% and 32%, respectively. For KN fiber, when the amounts of fiber increase, the flexural strengths decrease. Because of the forming ball problem, therefore, when higher amounts are used, the fiber is not well distributed which directly affects the flexural strength. In case of R-PET and PVA fibers, the flexural strength increases with increase in the amount of fiber.

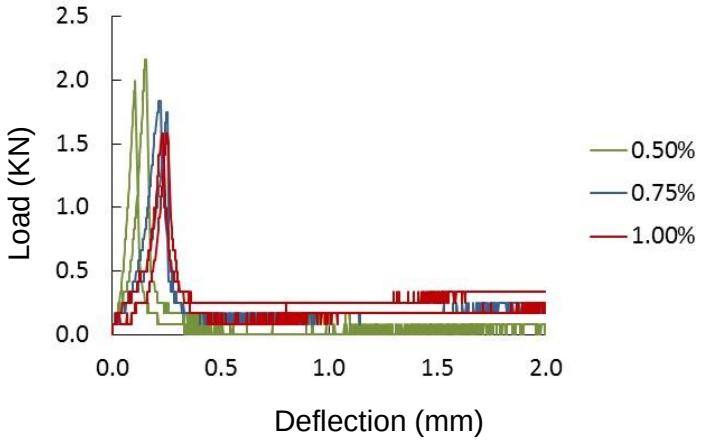

Figure 2.5: Load-midspan deflection curves of mortar specimens reinforced with knotted R-Nylon fiber

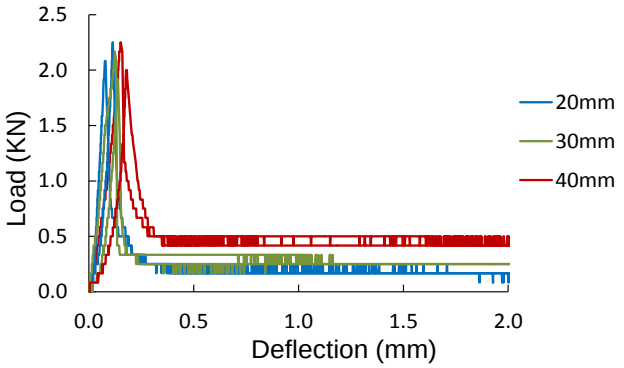

Figure 2.6: Load-midspan deflection curves of mortar specimens reinforced with straight R-Nylon fiber with 1.0% fiber fraction

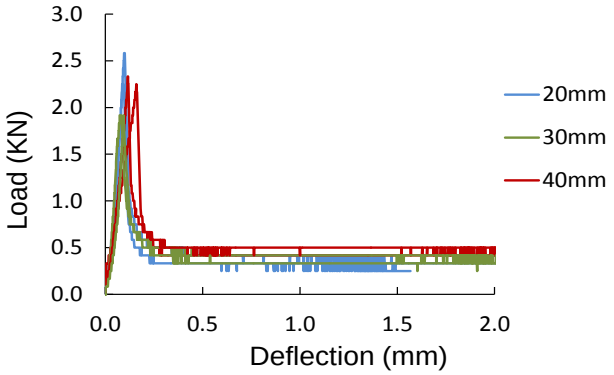

Figure 2.7: Load-midspan deflection curves of mortar specimens reinforced with straight R-Nylon fiber with 1.5% fiber fraction

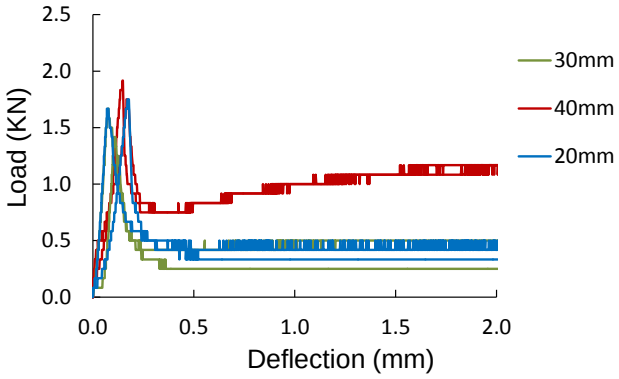

Figure 2.8: Load-midspan deflection curves of mortar specimens reinforced with straight R-Nylon fiber with 2.0% fiber fraction

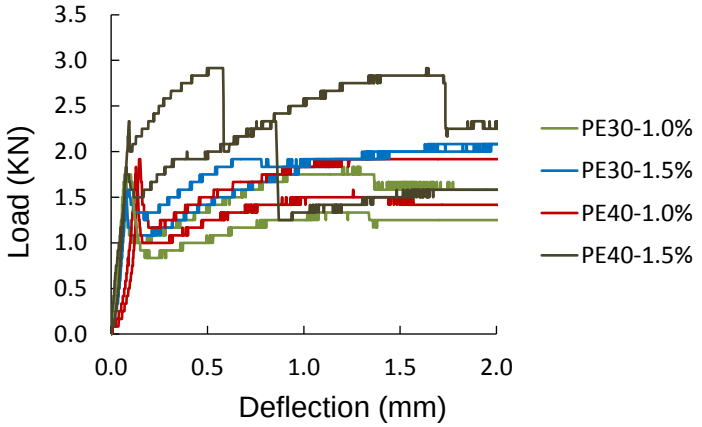

Figure 2.9: Load-midspan deflection curves of mortar specimens reinforced with R-PET fiber

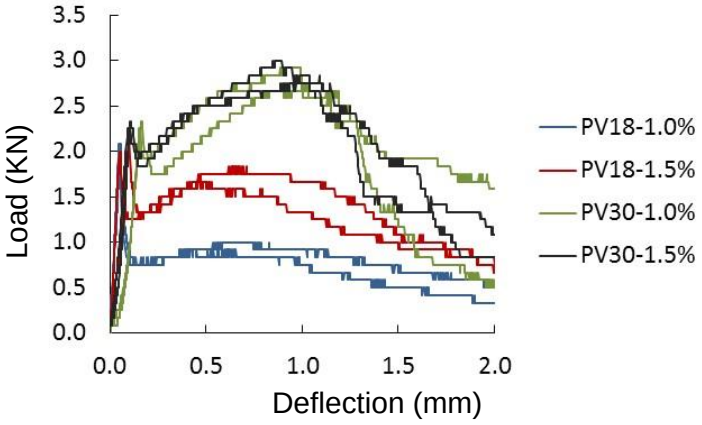

Figure 2.10: Load-midspan deflection curves of mortar specimens reinforced with PVA fiber

It can be clearly seen in Figures 2.5-2.10 that mortar reinforced with R-Nylon shows a significant reduction in load after the first crack. The second rising portion of the load-deflection curves prior to the second peak, corresponded to the hardening of bond-slip behavior. This phenomenon is very beneficial as long as the fiber does not break. The main reason why the R-PET fiber mortar is superior in the post peak load to other types of fiber may be concerned with the fiber geometry. The R-PET fiber used in this study had an embossed surface that significantly increases bond strength between the fiber and mortar. Kim et al. [40] carried out an investigation focusing on the effects of R-PET fiber geometry on bond behavior with hydrated cement matrix. In the mechanical bond test, the embossed fiber had considerably superior performance to the other types (straight and crimped), see Table 2.4. In case of the PVA fiber, strong chemical bond between the fiber and the hydrated cement matrix leads to break of the fiber rather than pullout from the hydrated cement matrix [13, 14]. When the specimens were subjected to bending load, PVA fiber tended to break before the bond failure, which caused lower post peak loads of the specimens mixed with PVA fiber lower than those

with R-PET fiber. In this study, the surfaces of the R-Nylon, R-PET and PVA fibers were examined after the bending test to analyze the frictional resistant force. As shown in Figure 2.11 (a), the R-Nylon fibers have no significant changes in their surfaces such as scratched; therefore, friction between the fiber surface and the cement matrix is poor, which leads to a decrease in frictional resistance to slippage. The R-PET surface was scratched as shown in Figure 2.11 (b), the bond strength was enhanced due to a mechanical anchorage effect in the embossed area. Moreover, since R-Nylon and R-PET fiber are softer than surrounding cement matrix, a part of their surfaces were peeled, which ascended the post peak load. In case of the PVA fiber, fragments of cement matrix were found on its surfaces, as shown in Figure 2.11 (c), due to strong chemical bond. When comparing the load-midspan deflection curves between SN-40-2.0 and PV-18-1.0 and 1.5, the post peak load of PV-18 gradually decreased with increase in the load applied, while the post peak load of SN-40-2.0 increased and was higher than that of PV-18-1.0 deflection. Even R-Nylon fiber surface smooth, however, 40 mm is long enough to prevent slippage due to anchor length. Such a bond improvement between fiber and matrix is essential for enhancing load carrying capacity of the composite due to improvement of stress transfer, from the matrix to fiber.

Table 2.4: Mechanical bond strength tested by Kim et al. [40]

Fiber geometry	**Straight**	**Crimped**	**Embossed**
Mechanical bond strength (MPa)	1.7	3.9	5.0

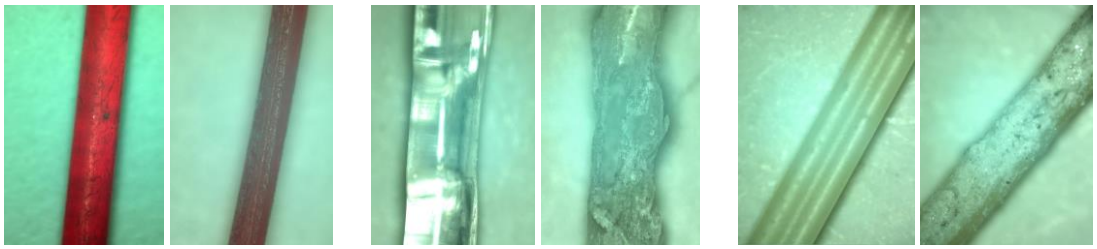

(a) Before After (b) Before After (c) Before After

Figure 2.11: The fiber surface before and after the flexural test. (a) R-Nylon fiber; (b) R-PET fiber; (c) PVA fiber (30 mm)

Table 2.5: Toughness indices and residual strength factors at 28 days

Specimen type	Toughness index			Residual strength factor	
	I_5	I_{10}	I_{20}	$R_{5,10}$	$R_{10,20}$
KN-40-0.5	1.61	1.82	2.42	4.20	6.02
KN-40-0.75	1.56	2.20	4.00	12.80	18.01
KN-40-1.0	1.91	3.27	6.21	27.20	29.43
SN-20-1.0	1.95	2.41	3.45	9.18	10.40
SN-20-1.5	2.40	3.38	5.23	19.50	18.50
SN-20-2.0	2.80	4.17	6.71	27.30	25.40
SN-30-1.0	1.97	2.91	4.79	18.80	18.80
SN-30-1.5	2.86	4.17	6.49	26.20	22.85
SN-30-2.0	3.05	4.23	7.29	23.60	30.61
SN-40-1.0	2.88	4.47	7.71	31.90	32.44
SN-40-1.5	2.49	4.25	7.80	35.18	35.42
SN-40-2.0	3.37	6.02	13.38	53.00	73.60
PE-30-1.0	3.15	5.99	13.03	56.94	70.34
PE-30-1.5	4.36	9.22	20.80	97.02	115.85
PE-40-1.0	5.07	11.29	25.60	124.26	143.10
PE-40-1.5	4.68	9.91	22.41	104.58	125.05
PV-18-1.0	2.77	4.62	8.74	37.00	41.21
PV-18-1.5	3.72	7.50	15.74	75.60	82.40
PV-30-1.0	5.09	11.33	20.58	124.74	92.50
PV-30-1.5	5.06	11.16	24.86	121.88	137.04

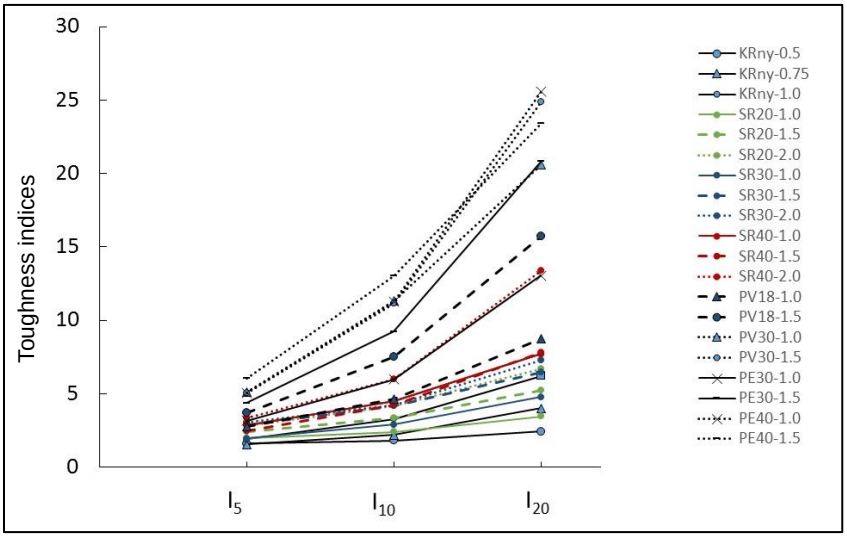

Figure 2.12: Toughness indices of fiber reinforced mortars

2.3.4 TOUGHNESS AND RESIDUAL STRENGTH

The toughness indices and residual strength factors are summarized in Table 2.5. It is obvious that the addition of the R-Nylon fiber to the mortar appears to afford outstanding improvements in toughness, especially for higher fiber fractions and greater length of fiber as shown in Figure 2.12. According to the embossed surface of the R-PET fiber, the R-PET fiber mortar performed outstanding post peak behavior; particularly the mortar with higher aspect ratio fiber (PE-40) exhibited higher toughness indices and residual strength factors. This implies that not only fiber length but also fiber geometries govern the bond characteristics between the fiber and cement matrix. The opposite result was obtained for the PVA fiber mortar: the smaller the aspect ratio of the fiber, the higher the post peak load. Redon and Li [15] conducted a pull out test, where two types of PVA fiber having 0.044 mm and 0.700 mm diameter were investigated. They found that the smaller diameter fiber broke before the full pullout length, while most of the larger diameter fibers were fully pulled out. Moreover, the larger diameter fiber embedded in the mortar decreased in its diameter according to abrasions. Therefore, the PV-30 mortar exhibited higher post peak load than the PV-18 mortar did. As evidenced by the results, the toughness and residual strength of KN fiber mortar presented worst performance because the fiber fraction is limited to low amount. Moreover, easily forming ball shape of KN fiber leads to poor fiber distribution, which directly affects toughness and residual strength of fiber reinforced mortar.

2.4 REFERENCES

1. ASTM C15557-03. "Standard test method for tensile strength and Young's modulus of fibers." *ASTM International*, West Conshohocken, PA.
2. ASTM C 1437. "Standard test method for flow of hydraulic cement mortar." *ASTM International*, West Conshohocken, PA.
3. ASTM C 39. "Standard test method for compressive strength of cylindrical compressive specimens." *ASTM Internatio*nal, West Conshohocken, PA.
4. ASTM C 1018. "Standard test method for flexural toughness and first-crack strength of fiber reinforced concrete." *ASTM International*, West Conshohocken, PA.
5. Wang, Y., Wu, H. C. and Li, V. C. (2000). "Concrete reinforcement with recycled fibers." *Journal of Materials in Civil Engineering*, 12(4), 314-319.
6. Hu, W., Yang, X., Zhou, J., Xing, H. and Xiang, J. (2013). "Experimental research on the mechanical properties of PVA fiber reinforced concrete." *Research Journal of Applied Science, Engineering and Technology*, 5(18), 4563-4567.
7. Karahan, O. and Atis, C. D. (2011). "The durability properties of polypropylene fiber reinforced fly ash concrete." *Materials and Design*, 32(2), 1044-1049.
8. Palmquist, S. M., Kintzel, E. and Andrew, K. (2011). "Scanning electron microscopy to examine concrete with carbon nanofibers." Proceedings of the 5th Pan American Conference for NDT, Cancun, Mexico.
9. Li, V. C. (1992). "A simplified micromechanical model of compressive strength of fiber-reinforced cementitious composites." *Cement and Concrete Composites*, 14, 131-141.
10. Fraternali, F., Farina, I., Polzone, C., Pagliuca, E. and Feo, L. (2013). "On the use of R-PET strips for reinforcement of cement mortars." *Composites B*. 46, 207-210.

11. Spadea, S., Farina, I., Carrafiello, A. and Fraternali, F. (2015). “Recycled nylon fibers as cement mortar reinforcement.” *Construction and Building Materials*, 80, 200-209.
12. Kim, J. H. J., Park, C. G., Lee, S. W., Lee, S. W. and Won, J. P. (2008). “Effects of the geometry of recycled PET fiber reinforcement on shrinkage cracking of cement-based composites.” *Composites B*, 39, 442-450.
13. Nematollahi, B., Sanjaya, J. and Ahmed Shaikh, F. U. (2015). “Tensile strain hardening behavior of PVA fiber-reinforced engineered geopolymer composite.” *Journal of Materials in Civil Engineering*, 27(10) (doi: 1943-5533.0001242).
14. Jewell, R. B., Mahboub, K. C., Robl, T. L. and Bathke, A. C. (2015). “Interfacial bond between reinforcing fibers and calcium sulfoaluminate cements: fiber pullout characteristics.” *ACI Materials Journal*, 112(1), 38-47.
15. Redon, C. and Li, V. C. (2001). “Measuring and modifying interface properties of PVA fibers in ECC matrix.” *Journal of Materials in Civil Engineering*, 13(6), 399-406.

CHAPTER 3

APPLICATION OF RECYCLED NYLON FIBER FROM WASTE FISHING NETS

3.1 INTRODUCTION

Reinforced concrete (RC) structures are prone to deterioration from corrosion damage, and such damage is particularly likely for structures near a marine environment. In the past few decades, concerns have arisen about the durability of RC structures, and civil engineers have been developing repair and strengthening methods. It has become ever more essential to strengthen new RC structures or partially deteriorated RC structures showing unsatisfactory performance. Obviously, the structural performance of RC structures improves as a result of repairs. However, choosing the proper repair materials and methods requires careful study: good repair affords enhanced functionality and performance, and restores and increases strength and stiffness. Furthermore, repairs prevent the ingress of corrosive agents to the steel surface by decreasing diffusivity and permeability, as well as making the concrete surface look good.

There are numerous techniques for repairing deteriorated RC beams. External post tensioning is one conventional technique, and it is used to increase the flexural strength of damaged RC structures. This technique has two main disadvantages: It is difficult to provide anchorage in post-tensioning strands, and the technique affects the lateral stability of the beam. Steel plate bonding is a widely used repair method; however, it increases the dead weight of the structure significantly and has difficulty in handling long-span beams. Moreover, external post-tensioning and bonded steel plates require measures against corrosion. FRP strengthening is an alternative to steel plate, to avoid problems related to corrosion. However, abrupt failure, lower ductility and high material costs have been identified as major drawbacks of this technique. Besides the above-mentioned, in case of steel and FRP external bond, plate debonding is the main problem of RC beams strengthening with steel plate and FRP sheet [1-6]. To address the problems associated with prevailing strengthening techniques, sprayed polymer cement mortar (SPCM) was developed to enhance flexural strength, stiffness and other aspects of structural performance, as well as to improve durability. Moreover, of these materials, cement-based ones are the most suitable for repairs [7]. A major advantage of this technique is that the SPCM adheres strongly to the intended surface due to the high spraying velocity. Even the inner layers are dense, so a well-compacted covering can be achieved. In contrast, for normal recasting, care must be taken, because previously applied layers of mortar need to gain strength before they set. Moreover, with hand-applied mortar, sometimes the vibrating apparatus cannot achieve access. Numerous studies on the repair of degraded RC structures have been addressed the performance of non-corroded RC beams repaired with polymer cement mortar [8], as well as overlay strengthening methods [9-11]. Less research has addressed SPCM repair for flexural corroded RC components that involves the replacement of corrosion-damaged concrete, and this is particularly true for research that compares different types of SPCMs.

In this study, recycled (R)-nylon fiber that was manually cut from waste fishing nets was added to the mixture (Figure 3.1 (a)). Orasutthikul et al. and Spadea et al. [12, 13] found that using R-nylon fiber not only improves the structural performance of fiber-reinforced mortar but also affords ecological and economic benefits. To compare the improvement in structural performance afforded by R-nylon fiber SPCM and two common types of SPCM (polyethylene (PE) fiber SPCM (see Figure 3.1 (b)) and non-fiber SPCM), four-point bending tests were conducted on a series of corrosion-damaged RC beams repaired with SPCM. Three work specifications were address: the removal of damaged concrete to a depth of 10 mm from the surface, the removal of all the cover concrete (26 mm deep), and the removal of concrete to a depth of 20 mm over the tensile reinforcements. Flexural behavior was investigated in terms of load carrying capacity, flexural stiffness and ductility as well as crack formation with bending tests that focused on the following test parameters: repair method, SPCM type and level of flexural reinforcement corrosion.

(a) R-nylon fiber

resulting mixture

(b) PE fiber

resulting mixture

Figure 3.1: Fiber mixed with polymer cement mortar: (a) SPCM containing R-nylon fiber; (b) SPCM containing PE fiber

3.2 EXPERIMENTAL PROGRAM

3.2.1 MATERIALS

A total of 38 RC beams, each 150 mm high by 100 mm wide by 900 mm long, were constructed in this study. The geometry and reinforcement of the beams are shown in Figure 3.2. For flexural reinforcement, two reinforcing bars of 10 mm were used as lower reinforcement and two reinforcing bars of 6 mm were used as upper reinforcement. Stirrups are arranged with 6-mm-diameter reinforcing bars at 90-mm intervals. The concrete was made with ordinary Portland cement (OPC), and its compressive strength was 33 MPa. The SPCM used in this study had almost the same compressive strength as the concrete that strengthens low-density polymer, and these SPCMs are categorized into three types (Table 3.1). The R-nylon fiber is considered as macro-fiber, the diameter is 0.35 mm and the length is 20 mm. In case of PE fiber, the length is 9 mm and it is considered as microfiber.

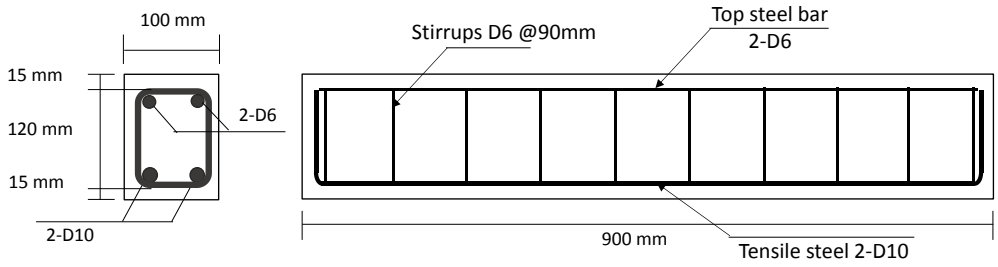

Figure 3.2: Reinforced concrete beam geometry and reinforcement details

Table 3.1: Properties of SPCM

SPCM type	Description	Fiber length (mm)	Fiber fraction by volume (%)	Compressive strength (MPa)	Modulus of Rupture (MPa)	Flow diameter (mm)
SPCM_NF	Non-fiber SPCM	-	-	35	5.3	157
SPCM_PE	SPCM with PE fiber	9	1.1	46	8.3	151
SPCM_RN	SPCM with R-nylon fiber	20	1.0	34.5	5.1	153

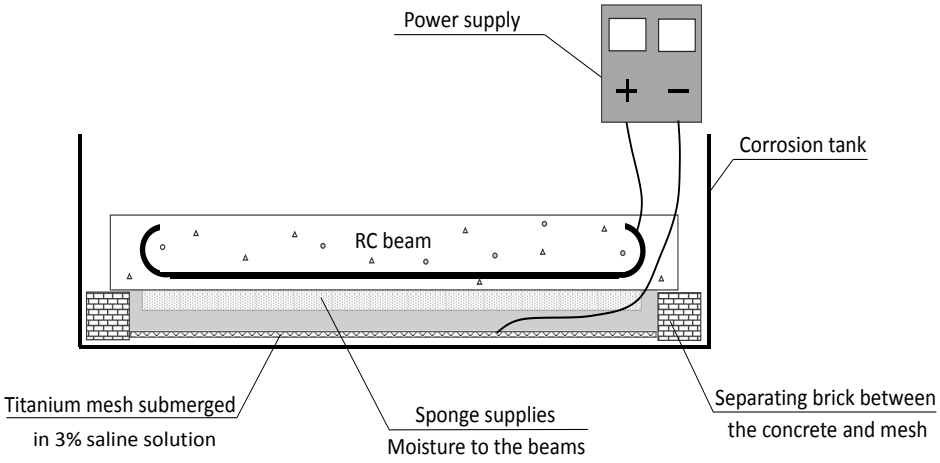

(a)

(b)

Figure 3.3: Accelerated corrosion system

3.2.2 ACCELERATED CORROSION

Since the objective of this study is to evaluate the effectiveness of SPCM in repairing corroded RC beams, 34 RC beams were first corroded by an accelerated corrosion system, as illustrated in Figure 3.3.

The specimens were categorized by three levels of corrosion.
Level A: no corrosion (or control beam)
Level B: $0 < r \leq 10\%$
Level C: $10\% < r \leq 18\%$
Level D: $18\% < r \leq 25\%$

Where r = % mass loss of tensile steel

After finishing accelerated corrosion, splitting cracks were observed in concrete cover along the alignment of the tensile steel, as shown in Figure 3.4.

(a)

(b)

Figure 3.4: Beams after finishing accelerated corrosion: (a) side of the beam; (b) bottom of the beam

3.2.3 REPAIR METHODS AND PROCEDURES

In this experiment, SPCM was applied to the bottom of the corrosion-damaged beams. First, polymer cement containing acrylic powder and water were mixed by mixing machine for about 1 minute. The water-to-binder ratio was 0.2. After that (in the case of adding fiber), the fiber was put into the mixing machine for 2 more minutes of mixing. The mixture was put into a

pump hopper and then sprayed on the bottom of the corrosion-damaged RC beam, as shown in Figure 3.5. In this study, three repair methods were investigated.
Repair method 1 – 10-mm application of SPCM (Figure 3.6 (a)): Prior to the SPCM repair, damaged concrete was removed to a depth of about 10 mm. The old concrete was removed by using a diamond cutter, and then the SPCM was applied to the tensile surface.
Repair method 2 – SPCM application after removal of all the covering concrete (Figure 3.6 (b)): The corrosion-damaged concrete was removed up to the location of tensile reinforcement by using a hammer and a wedge, and then the SPCM was applied.
Repair method 3 – SPCM application after the removal of concrete to a depth of 20 mm beyond the tensile reinforcement (Figure 3.6(c)): The bottom surface of the concrete cover was first cut by a diamond cutter, and then a hammer and a wedge were used to clear the concrete from that surface.

In all the repair methods, the corroded tensile reinforcement was not replaced. Of the three methods, method 1 is the most economical; however, because the concrete was removed only to a depth of 10, there were leftover corrosive agents as well as corrosion cracks, and the bond between the concrete and the steel bars that had been lost as a result of rusting was not restored. In method 2, the damaged concrete was removed to whole covering thickness. Such removal can prevent the ingress of corrosive agents; however, some chemical agents remain in the concrete over the tensile reinforcement, and the lost bond is not fully restored. Because it overcomes the main shortcomings of the above two methods, repair method 3 is the best choice for protecting steel against further corrosion. However, it is more costly; therefore, this method is usually used only for beams with severe corrosion.

Figure 3.5: Spraying polymer cement mortar

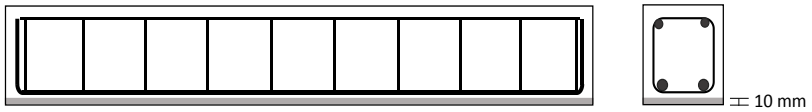

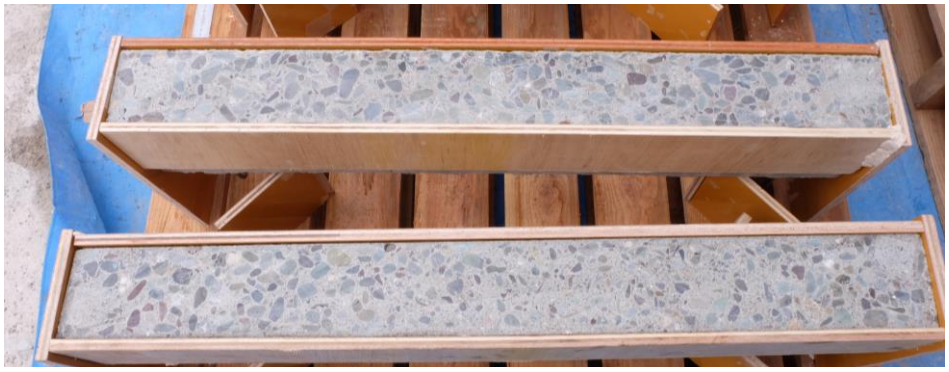

(a) Repair method 1

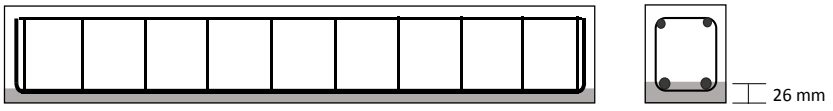

(b) Repair method 2

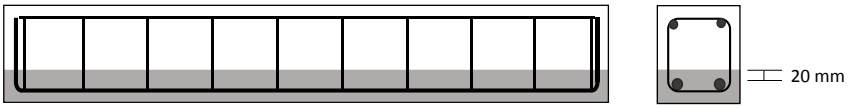

(C) Repair method 3

Figure 3.6: Repair methods

3.2.4 LOADING TEST

In this study, four-point bending tests were conducted, as shown in Figure 3.7. Four linear variable differential transformers (LVDTs) were used to measure deflection; two were installed at the midspan and the other two were installed at each support. A total of 6 strain gauges were glued at the mid-span, with 4 installed along the side of the beam and 2 installed at the top and bottom of the beam, respectively, to measure the strain.

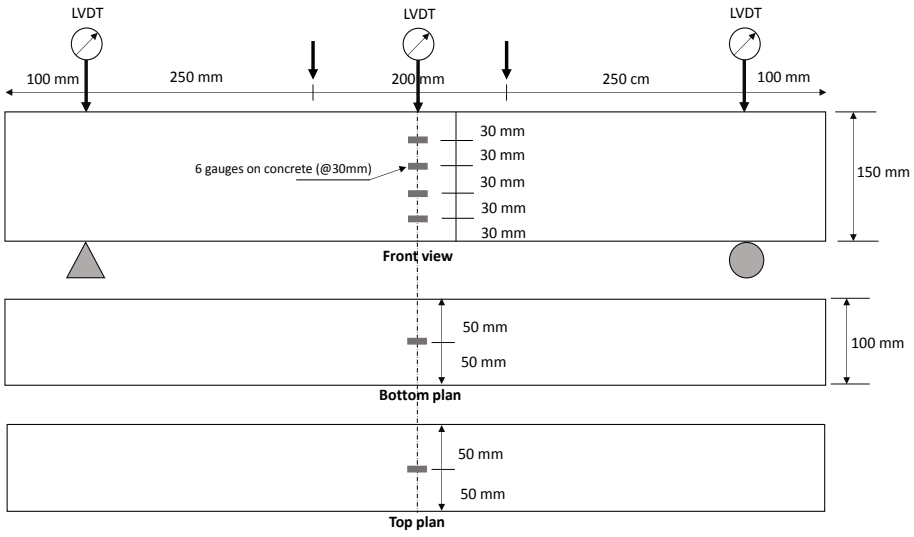

Figure 3.7: Four point bending test setup

3.3 EXPERIMENTAL RESULTS

3.3.1 LOAD CARRYING CAPACITY

The yield and ultimate loads of the repaired beams with different repair methods and SPCM types are presented in Table 3.2. The results show that the change in load carrying capacity of the repaired beams differed depending on the repair method and the SPCM type. Figure 3.8 shows the percent improvement in ultimate load for the RC beams repaired with SPCM, with 0% indicting the non-deteriorated, non-repaired control beams. The results show that the load carrying capacity of the corroded RC beams repaired with fiber-containing SPCM (either type of fiber) tended to be higher than those of beams repaired with non-fiber-containing SPCM. The enhancement resulting from the inclusion of fibers could be due to delaying crack propagation and improving bond strength. Addition of fiber improves not only bond strength at ultimate load, but bond slip value at the maximum bond strength as well [14]. For non-damaged RC beams strengthened with method 1 in combination with SPCM_PE, the ultimate load averagely increased by 11.1%. For beams with corrosion level B, repair method 2 exhibited the highest effectiveness in restoring load bearing capacity, especially when SPCM_PE was used. This combination was able to enhance the ultimate load by almost 9% compared with the non-repaired, non-damaged RC beams. In the case of corrosion level C, method 3 was the most suitable for strength recovery, with this method resulting in an average increase of 5.71% in the ultimate load when SPCM_RN was used. Moreover, it was found that, for the beams with corrosion level D, load carrying capacity recovering effectiveness of the SPCM repair technique is insufficient.

Table 3.2: Types of specimens and test results

Corrosion level	Specimen	Mass loss rate (%)	Repairing method	Yielding load (Y) (kN)	(ΔY%)	Ultimate load (U) (kN)	(ΔU%)
A	A0 (1)	-	-	42.36		48.36	
	A0 (2)	-		43.36		53.87	
	A1-PE (1)	-	1	48.20	10.90	56.54	11.1
	A1-PE (2)	-		46.86		57.04	
B	B0 (1)	7-9	0	38.02		46.36	
	B0 (2)	7-9		40.69		52.37	
	B1-PE (1)	7-9	1	43.36	1.70	56.20	3.88
	B1-PE (2)	7-9		36.69		46.36	
	B2-NF (1)	7-9	2	36.69	-4.65	49.20	6.93
	B2-NF (2)	7-9		38.36		56.37	
	B2-PE (1)	7-9	2	46.20	9.12	55.37	12.50
	B2-PE (2)	7-9		39.69		55.70	
	B2-RN (1)	7-9	2	41.36	1.07	51.70	2.87
	B2-RN (2)	7-9		38.19		49.86	
	B3-PE (1)	7-9	3	44.69	20.56	54.20	6.58
	B3-PE (2)	7-9		50.20		51.03	
C	C0 (1)	13-16	-	38.69		45.86	
	C0 (2)	13-16		35.52		45.03	
	C1-PE (1)	13-16	1	34.85	-3.60	41.86	-4.04
	C1-PE (2)	13-16		36.69		45.36	
	C2-NF (1)	13-16	2	29.18	-9.66	42.03	-3.85
	C2-NF (2)	13-16		37.86		45.36	
	C2-PE (1)	13-16	2	46.53	19.55	50.36	7.51
	C2-PE (2)	13-16		42.19		47.36	
	C3-NF (1)	13-16	3	35.36	-11.22	48.20	-1.83
	C3-NF (2)	13-16		30.52		41.03	
	C3-PE (1)	13-16	3	40.69	16.63	46.86	13.03
	C3-PE (2)	13-16		45.86		55.87	
	C3-RN (1)	13-16	3	40.19	6.74	54.70	18.90
	C3-RN (2)	13-16		39.02		53.37	
D	D0 (1)$_1$	23-25	-	25.85		40.19	
	D0 (2)	23-25		24.35		33.85	
	D2-NF (1)	19-22	2	25.85	2.99	40.36	12.63
	D2-NF (2)	19-22		25.85		43.03	
	D2-PE (1)	19-22	2	33.69	27.91	38.36	0.69
	D2-PE (2)	23-25		30.52		36.19	
	D3-PE (1)	23-25	3	29.69	21.59	36.69	11.49
	D3-PE (2)	19-22		27.51		45.86	

Note: the specimen name is noted as "corrosion level" followed by "repair method-SPCM type".

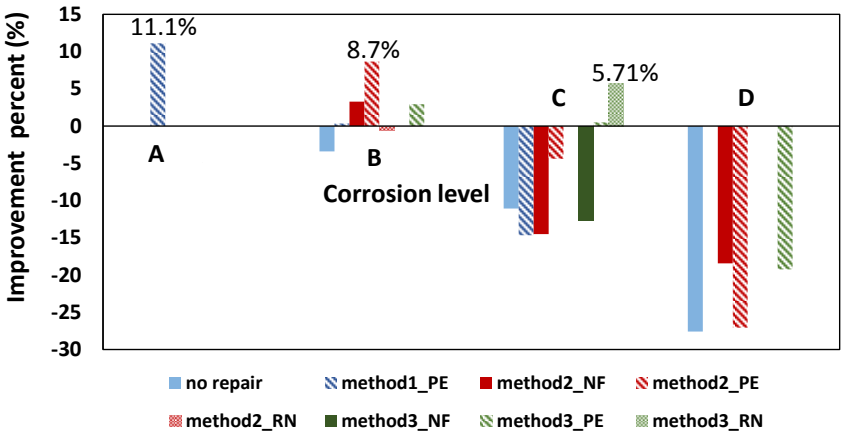

Figure 3.8: Effect of SPCM on load carrying capacity

Table 3.3: Ductility indices of repaired beams

Corrosion level	Specimen	Repairing method	Energy ductility (D_E)	Displacement ductility (D_D)
A	A0	-	7.59	4.00
	A1-NF	1	6.19	3.72
B	B0	0	11.36	6.47
	B1-PE	1	9.96	5.98
	B2-NF	2	12.05	6.62
	B2-PE	2	9.56	5.43
	B2-RN	2	37.53	19.55
	B3-NF	3	5.18	3.43
C	C0	-	8.38	4.90
	C1-PE	1	6.28	4.04
	C2-NF	2	7.48	4.36
	C2-PE	2	4.78	3.33
	C3-NF	3	11.36	5.99
	C3-PE	3	4.52	3.05
	C3-RN	3	28.80	13.85
D	D0	-	13.10	7.11
	D2-NF	2	14.20	7.30
	D2-PE	2	6. 67	4.17
	D3-PE	3	21.35	9.38

3.3.2 DUCTILITY

Table 3.3 presents the ductility indices of the beams repaired with different methods and SPCM types. From the results in Figure 3.9, both indices of ductility show the same trend, with ductility differing according to the repair method and SPCM type at a given corrosion level. As expected, most of the beams repaired with SPCM_PE exhibited lower ductility than the control beams. For the beams at corrosion levels B and C, the ductility indices for SPCM_PE, both displacement-based and energy-based, were the greatest for method 1, followed by method 2 and method 3.For severe corroded reinforcement (level D), it was found that some parts of reinforcement have localized reduction of cross section which significantly affected the structural behavior and performance of repaired RC beams. Therefore, it cannot be clearly seen the effects of repaired methods on the ductility.

The R-nylon SPCM repaired beams exhibited excellent ductility indices, and these were the best of any SPCM type. It is reasoned that R-nylon fiber which is large fiber, is beneficial in transferring tensile stresses in the member by delaying fiber pull-out and restraining macro-crack propagation. The control of crack growth during loading slows the overall flexural failure of the repaired beams; therefore, the R-nylon SPCM repaired beams show greater deformation than the beams repaired with either of the two other SPCM types. For the specimens repaired with SPCM_PE, the fiber can bridge microcracks, and since for a given volume these fibers are much closer together and disperse large cracks as many fine cracks. Moreover, PE fiber is short and therefore may be pulled out or rupture after macro-cracks are formed, thus providing a little ductility. The illustration of different sizes of fibers on crack bridging is shown in Figure 3.10. In contrast, the beams repaired with SPCM_NF exhibited higher ductility than those repaired with SPCM_PE, due to the rapid growth of flexural cracks and the presence of many wide cracks. Consequently, large deflection occurred.

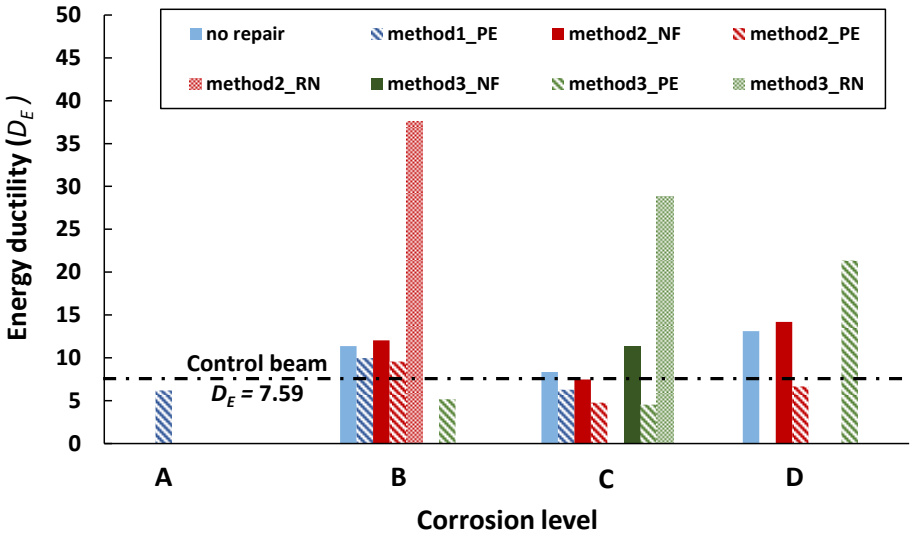

(a)

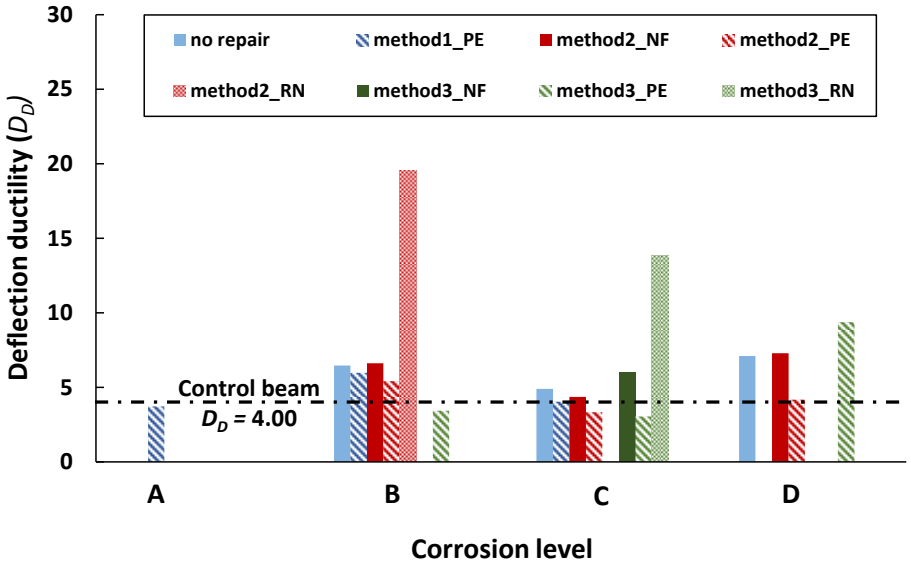

(b)

Figure 3.9: Ductility for reinforced concrete beams repaired with SPCM: (a) energy ductility; (b) deflection ductility

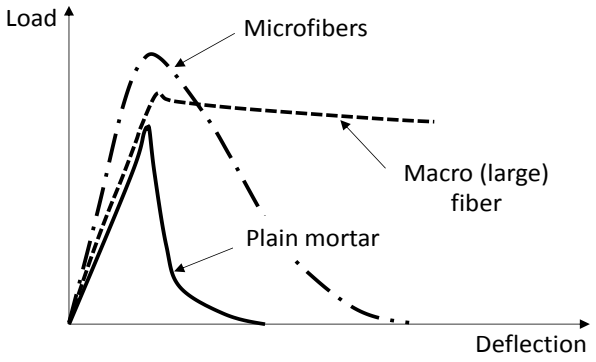

Figure 3.10: Typical load vs deflection curves for the fiber reinforced mortar

3.3.3 FLEXURAL STIFFNESS

The load-midspan deflection curves of the control beams and the beams repaired with SPCM are shown in Figure 3.11 (a) to (d). The midspan deflection was averaged a pair of measured values of two LVDT's at the midspan. The control beam means non-deteriorated and non-repaired beam. As shown in Figure 1.6, the load-deflection curve can be divided into three phases. In the first phase, OA, the relationship between load and deflection is linear. In the

second phase, AB, the relationship between load and deflection is roughly linear and the slope of the curve is less than in the first phase. In the third phase, also called the yield phase, BC, the deflection increases rapidly. As shown in Figure 3.11 (a), the flexural stiffness of the non-damaged beams strengthened with method 1 in combination with SPCM_PE is larger than that of control beam during three phase. Figure 3.11 (b) shows the flexural stiffness of the RC beams in corrosion group B. The flexural stiffness of the beams repaired with method 2 in combination with SPCM_PE showed an increase similar to that of the beams repaired by method 3 with SPCM_PE. For method 2, the damaged concrete over the tensile steel was not removed, and this might have been beneficial, as the corrosion product increases the surface roughness of the reinforcing steel, which results in improved bonding capacity for a mildly corroded steel bar [15]. However, this is regarded as a short-term improvement. At corrosion level C, as shown in Figure 3.11 (c), the beams repaired with method 3 showed high stiffness, especially when SPCM_PE was used. The flexural stiffness of the beams repaired with SPCM_NF increased to achieve roughly the flexural stiffness of the non-repaired beams. Moreover, these two graphs make it obvious that, in the third phase, the beams repaired with SPCM_RN provided ductility that was excellent and that was superior to those of the other SPCM types. In case of corrosion level D, the flexural stiffness of all repaired beams was improved compared with non-repaired beam, especially the beams repaired with method 3 in combination with SPCM_PE. However, load carrying capacity of all repaired beams is lower than that of control beam in the third phase, as shown in Figure 3.11 (d).

When SPCM type is considered, it is found that the beams repaired with SPCM containing fibers, exhibited higher stiffness than the non-fiber SPCM and non-repaired beams. It is considered that the fibers played the important role of bridging cracks such as to allow for the cracks to be distributed uniformly throughout the tension zone, which not only delays the development of major cracks in the SPCM but also disperses severe cracks as much smaller cracks. For the beams repaired with SPCM_PE, at any applied load, PE fiber can bridge microcracks and thus significantly enhance the tensile strength and stiffness of repaired beams. Moreover, as mentioned earlier in the ductility part, PE fiber tends to be pulled out or ruptures after macro-cracks are formed. Therefore, at any applied load, the deflection of the beams repaired with SPCM containing PE fiber, was reduced significantly, thereby increasing the stiffness of the repaired beams. In case of the beams repaired with SPCM containing R-nylon fiber, the fibers exert closing traction on the macro-crack surface due to pullout resisting force, consequently slow down crack growth, which results in improved both flexural stiffness and especially ductility of the repaired RC beams. Therefore, in the third phase, it is obvious that the beams repaired with SPCM_RN provided ductility that was excellent and that was superior to those of the other SPCM types.

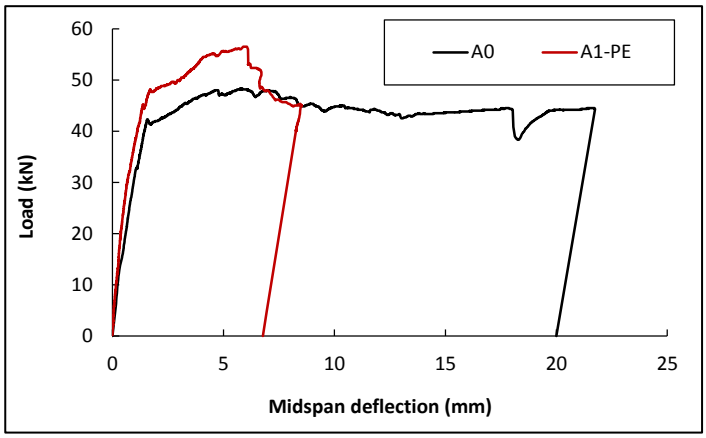

(a) Corrosion level A

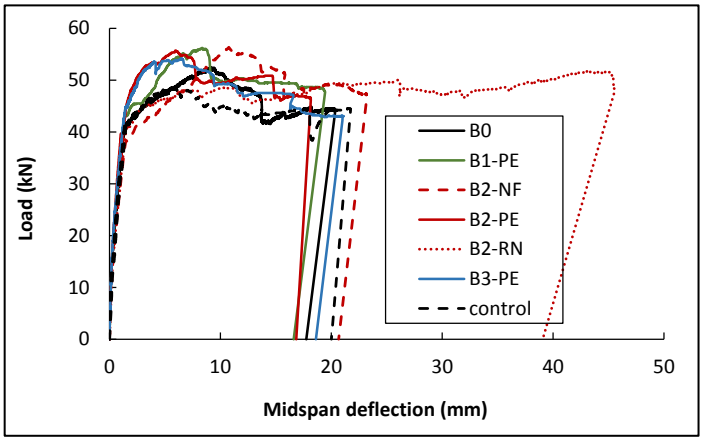

(b) Corrosion level B

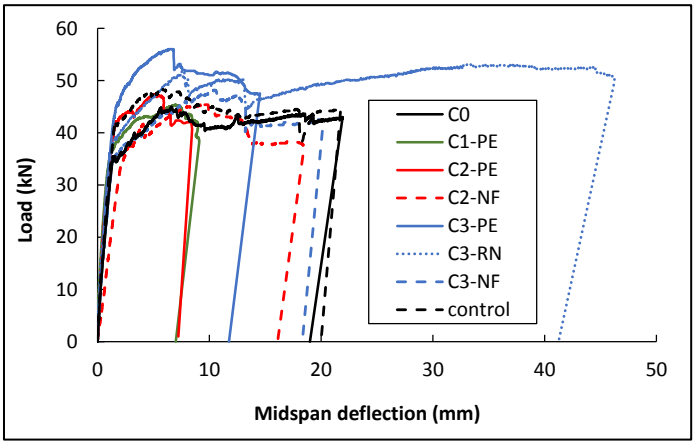

(c) Corrosion level C

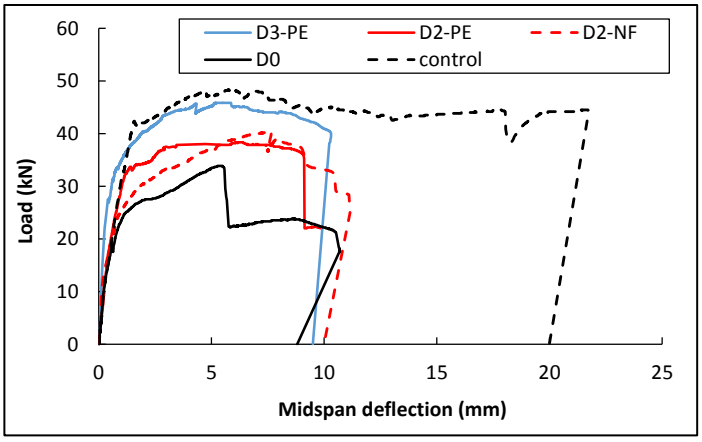

(d) Corrosion level D

Figure 3.11: Load vs midspan deflection of beams repaired with different methods and PCM types

3.3.4 CRACK FORMATION

Generally, the flexural stress of RC beams is transferred to SPCM through the SPCM-concrete interface. The debonding failure of SPCM can initiate if the SPCM-concrete bond stress is larger than bond strength. Therefore, the design procedure for SPCM to repair corrosion damaged RC beam should avoid this kind of failure to optimize the efficiency of repair material and method. Figure 3.12 shows the crack formation of non-damaged RC beams strengthened with method 1 in combination with SPCM_PE, a conventional flexural mode of failure was observed followed by crushing of concrete at the compression face. In contrast, for damaged RC beams with corrosion levels B and C, regarding the lost bond between concrete and tensile steel, it was observed that number of flexural cracks decreased as the splitting crack width was growing larger, finally resulted in peeling of concrete cover, as shown in Figure 3.13. For the beams repaired with method 2, which damaged concrete is removed whole concrete covering, flexural crack formed gradually, followed by concrete or SPCM peeling at the midspan area, as shown in Figure 3.14 (a) and (b). In the section between two primary cracks, the elongation of tensile steel is restrained by bond between concrete or SPCM and tensile steel which is known as local bond stress, as illustrated in Figure 3.14 (c) (Goto 1971; Nayal et al. 2006; Satoh and Kodama 2005; Zhang et al. 2011). After yielding of tensile steel, the bond stress transfer at the boundary surface rapidly increases and reaches bond strength, subsequently, peeling occurs. In addition, it was observed that, the spacing between the primary flexural cracks is between 65 – 90 mm, in this experiment. In case of the beams repaired with method 3 in combination with SPCM_NF and SPCM_PE, flexural cracks were observed accompanied by concrete crushing in the compression zone, no horizontal crack can be observed, as shown in Figure 3.15 (a) and (b). For the beams repaired with SPCM_RN, large deformation of the beams occurred as a result of high ductility, which resulted in intermediate crack debonding of SPCM_RN, as shown in Figure 3.15 (c). According to experiment observation, debonding occurred at load application points which is nearest to constant moment zone and shear flexure

zone as shown in Figure 3.16. The SPCM_RN-concrete interface shear stress occurs as a consequence of the tension stiffening effect between SPCM_RN and reinforcement. When the repaired beam undergoes very large deflection, once the transferred shear force is equal to or greater than the bond strength between concrete and SPCM_RN, this leads to debonding.

It was found that the beams repaired with non-fiber containing SPCM showed a rapid growth of cracks as brittle manner, and spalling of SPCM was observed, as shown in Figure 3.17. Moreover, number of severe cracks were observed to be higher, and total number of cracks were observed to be lower than those repaired with SPCM containing fibers because the fibers dispersed severe cracks as much smaller cracks.

Figure 3.12. Crack formation of non-damaged beam strengthened with method 1 in combination with SPCM_PE

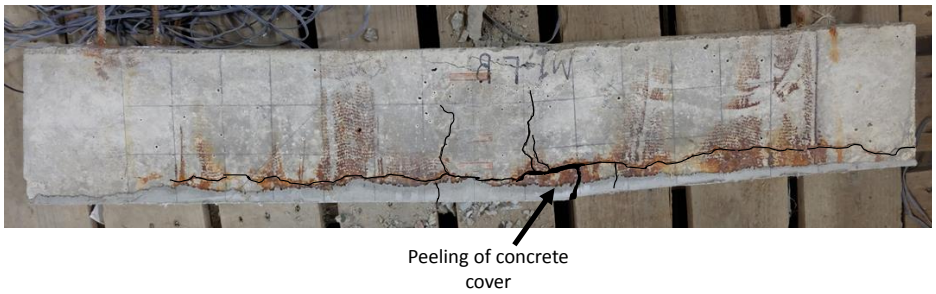

Figure 3.13. Typical crack formation of the corroded beams repaired with method 1

(a)

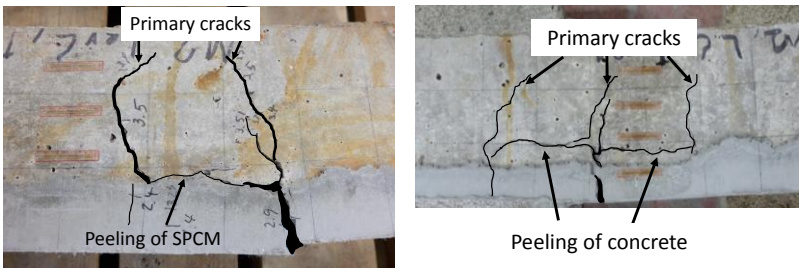

(b)

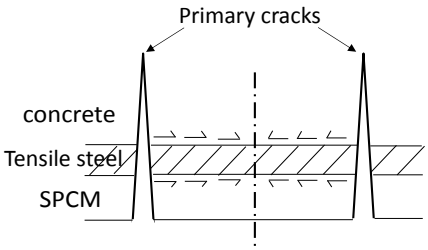

(c)

Figure 3.14. Crack formation of the beam repaired with method 2: (a) Typical central peeling of the beam repaired with method 2; (b) Peeling of SPCM or concrete at the midspan; and (c) Primary cracks formation of the beams repaired with method 2

(a) Beam B3-PE

(b) Beam C3-NF

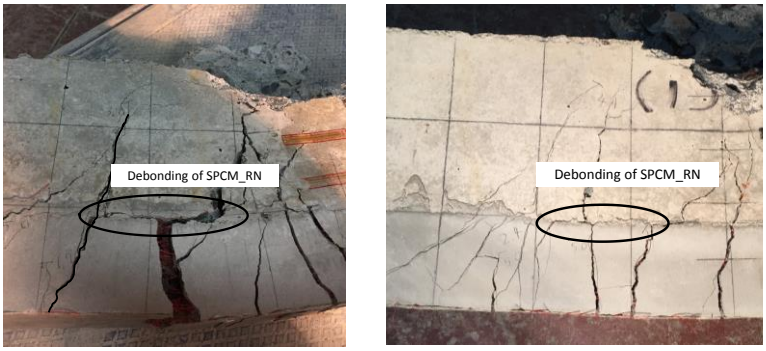

(c)

Figure 3.15. Crack formation of the beams repaired with method 3: (a) The beam repaired with SPCM containing PE fiber; (b) The beam repaired with non-fiber containing SPCM; and (c) Peeling of SPCM containing R-nylon fiber

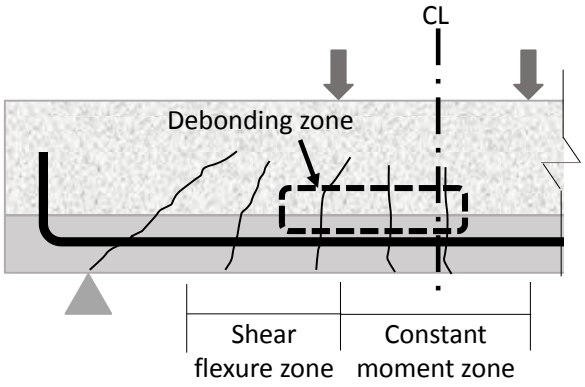

Figure 3.16. Illustration of debonding zone

Figure 3.17. Spalling of non-fiber containing SPCM

3.3.5 NEUTRAL AXIS

In this study, all the beams, excluding the beams in corrosion group A, were subjected to artificial corrosion damage on the tensile reinforcement causing debonding in reinforcing steel and horizontal crack along longitudinal steel bars. As the repaired beams consist of two materials, a high repair effect is indicated only if there is perfect bonding between the interfaces of the materials. The strain distribution along mid-span cross-section of the beams are present in Figure 3.18 (a) – (f).

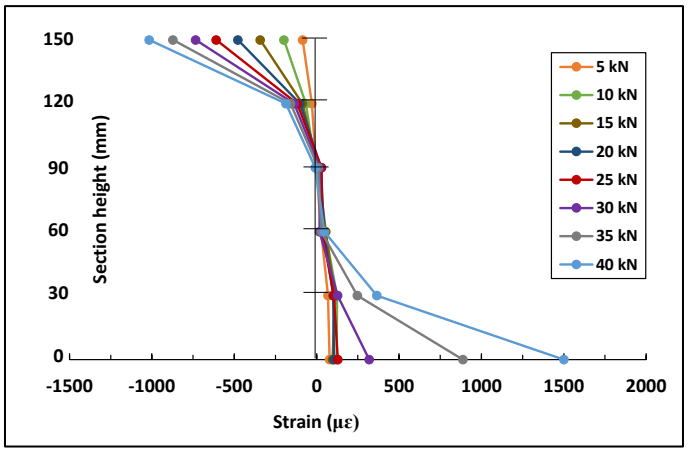

(a) Beam A1-PE

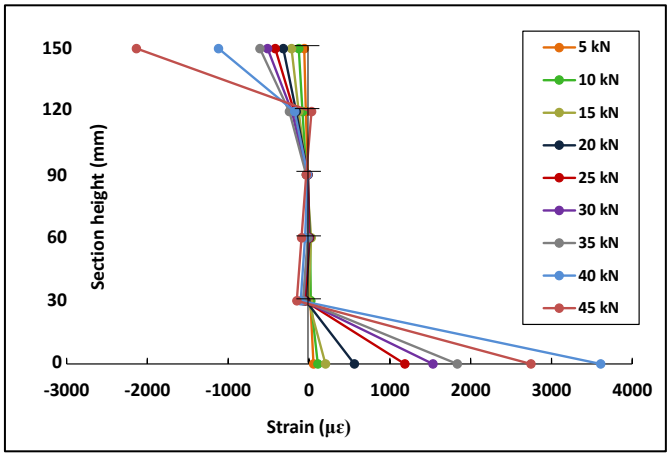

(b) Beam B1-PE

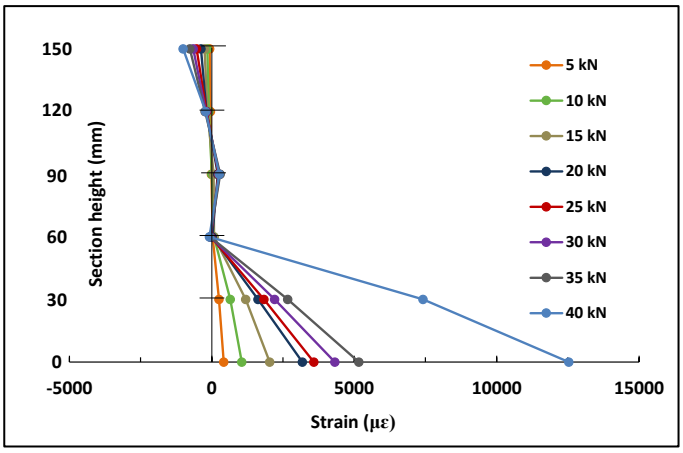

(c) Beam B2-NF

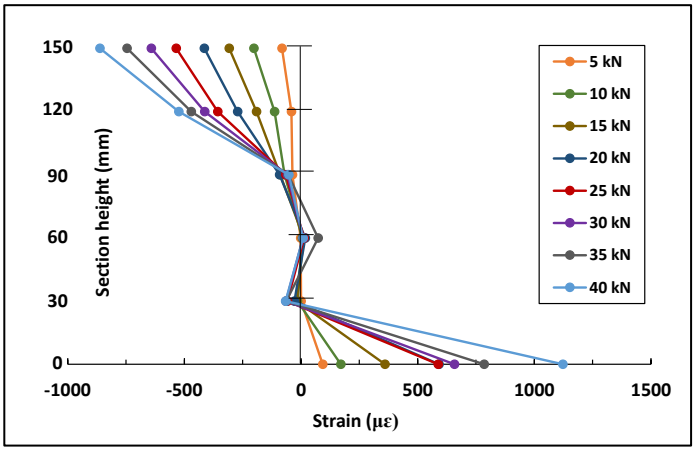

(d) Beam C2-PE

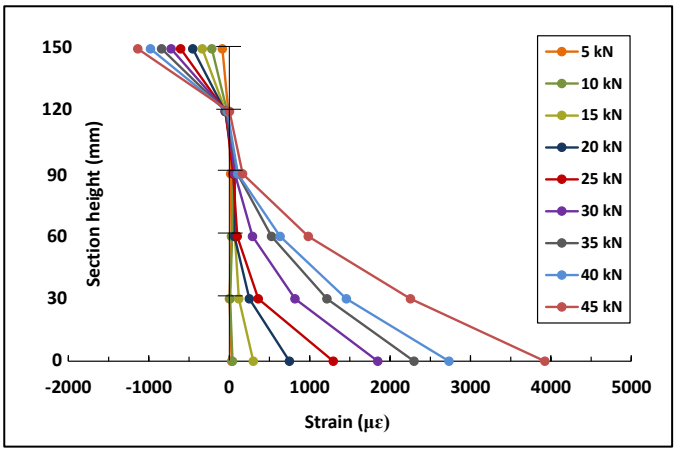

(e) Beam C3-PE

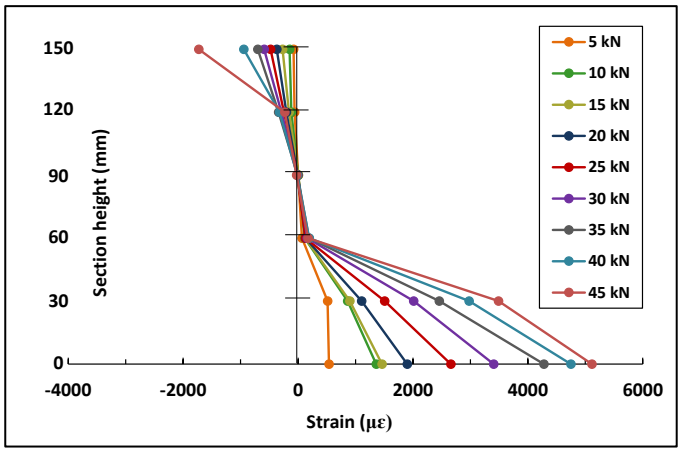

(f) Beam C3-RN

Figure 3.18: Strain distribution along midspan cross section

3.4 SUMMARY

The effectiveness of SPCM repair technique was investigated for structural performance recovery of corrosion damaged RC beams. The flexural behavior was analyzed in terms of load carrying, flexural stiffness and ductility as well as crack formation with bending tests that focused on the following test parameters: repair method, SPCM types and level of flexural reinforcement corrosion. Table 3.4 presents the recommendation of SPCM repair technique on corrosion damaged RC beams.

Table 3.4: Recommendation of SPCM repair technique on corrosion damaged RC beams

Corrosion level	Repair/strengthening method	SPCM type	Description
Level A (no corrosion)	Method 1	SPCM_PE	Upgrading structural performance of new RC beam (ex. Load carrying capacity and flexural stiffness) as well as prevent ingression of corrosive/aggressive agents.
Level B (0% <r≤ 10%)	Method 2/3	SPCM_PE/SPCM_RN	Method 2: Recover load carrying capacity and flexural stiffness as well as can be a better choice in terms of economic efficiency. Method 3: Recover load carrying capacity and flexural stiffness, however, ductility decreases. More costly
Level C (10% <r≤18%)	Method 3	SPCM_PE/SPCM_RN	SPCM_RN: Recover load carrying capacity and flexural stiffness as well as provide excellent ductility. SPCM_PE: Recover load carrying capacity, however, ductility decreases.
Level D (18% <r≤25%)	-	-	This corrosion level, only replace with SPCM is not sufficient for flexural strength recovery.

3.5 REFERENCES

1. Oehlers, D. J. (1992). "Reinforced concrete beams with plates glued to their soffits." Journal of Structural Engineering, 118(8), 2023-2038.
2. Saadatmanesh, H., and Malek, A. M. (1998). "Design guidelines for flexural strengthening of RC beams with FRP plates." Journal of Composites for Construction, ASCE, 2(4), 158-164.
3. Varastehpour, H., and Hamelin, P. (1997) "Strengthening of concrete beams using fiber-reinforced plastics." Materials and structures, 30, 160-166.
4. Ziraba, Y. N., Baluch, M. H., Basunbul, I. A., Sharif, A. M., Azad, A. K., and Al-Sulaimani, G. J. (1994). "Guidelines toward the design of reinforced concrete (RC) beams with external plates." ACI Structural Journal, 91(6), 639-646.
5. Wu, Z. S., Yuan, H., Kojima, Y., and Ahmed, E. (2005). "Experimental and analytical studies on peeling and spalling resistance of unidirectional FRP sheets bonded to concrete." Composites Science and Technology, 65(7-8), 1088-1097.
6. Wu, Z. S., and Niu, H. D. (2000). "Study on debonding failure load of RC beams strengthened with FRP sheets." Journal of Structural Engineering, 46A(3), 1431-1441.
7. Jumaat, M. Z., Kabir, M. H. and Obaydullah M. (2006). "A review of the repair of reinforced concrete beams." *Journal of Applied Science Research*, 2(6), 317-326.
8. Park, S. K. and Yang, D. S. (2005). "Flexural behavior of reinforced concrete beams with cementitious repair materials." *Materials and Structures*, 38, 329-334.
9. Rashid, K., Ueda, T., and Zhang, T. (2016). "Study on shear behavior of concrete-polymer cement mortar at elevated temperature." Civil Engineering Dimension, 18(2), 93-102.
10. Mizukoshi, M., Yamamoto, H., and Higashiyama, H. (2012). "Shear capacity evaluation of rc beams strengthened by underside overlay method using high-performance polymer cement mortar." Cement Science and Concrete Technology, 66(1), 584-591.
11. Satoh, K., and Kodama, K. (2005) "Central peeling failure behavior of Polymer Cement Mortar Retrofitting of Reinforced Concrete Beams." *Journal of Materials in Civil Engineering, ASCE*, 17(2), 126-136.
12. Orasutthikul, S., Unno, D., Yokota, H. and HASHIMOTO, K. (2017). "Effectiveness of recycled nylon fiber as a reinforcing material in mortar." *Journal of Asian Concrete Federation*, 2(2), 102-109.
13. Spadea, S., Farina, I., Carrafiello, A., and Fraternali, F. (2015) "Recycled nylon fibers as cement mortar reinforcement." *Construction and Building Materials*, 80, pp. 200-209.
14. Ali, A., Iqbal, S., Holschemacher, K., and Bier, T. A. (2017). "Bond of reinforcement with normal weight fiber reinforced concrete" *Periodica Polytechnica Civil Engineering,* 61(1), 128-134.
15. Lee B. D., Kim K. H., Yu H. G. and Ahn, T. S. (2004). "The effect of initial rust on the bond strength of reinforcement." *KSCE Journal of Civil Engineering*, 8(1), 35-41.
16. Goto, Y. (1971). "Cracks formed in concrete around deformed tension bars." *ACI Journal*, 68(4), 244-251.
17. Nayal, R., and Rasheed, H. A. (2006). "Tension stiffening model for concrete beams reinforced with steel and FRP bars." Journal of Materials in Civil Engineering, ASCE, 18(6), 831-841.
18. Zhang, D., Ueda, T., and Furuuchi, H. (2011) "Intermediate crack debonding of polymer cement mortar overlay-strengthened RC beam." *Journal of Materials in Civil Engineering,* ASCE, 23(6), 857-865.

CHAPTER 4

CASE STUDY: REPAIR PROGRAM CONSIDERING DURABILITY

4.1 INTRODUCTION

In order to obtain a durable concrete structure, all concerned processes for making the structure must be satisfactory. The mentioned processes include structural analysis, structural design and detailing, selection of materials and mix proportion, methods and control of the quality of construction and also maintenance plans.

In this study the structural behavior and performance of corroded RC beams with same corrosion level but different repairing time were compared, as illustrated in Figure 4.1.
The repaired beams are divided into two groups that are:

Group 1: the beams were corroded until corrosion level B (T_1) was achieved, then they were repaired with method 2 and 3. After that, they were corroded again until reached to the corrosion level C.
Group 2: the RC beams were corroded until corrosion level C was achieved (T_2), then they were repaired with method 2 and 3.

SPCM type that we used in this case study is SPCM containing PE short fiber. After that, those beams were investigated the structural behavior and performance by conducting four-point bending tests. The load carrying capacity, flexural stiffness, ductility and crack formation were analyzed.

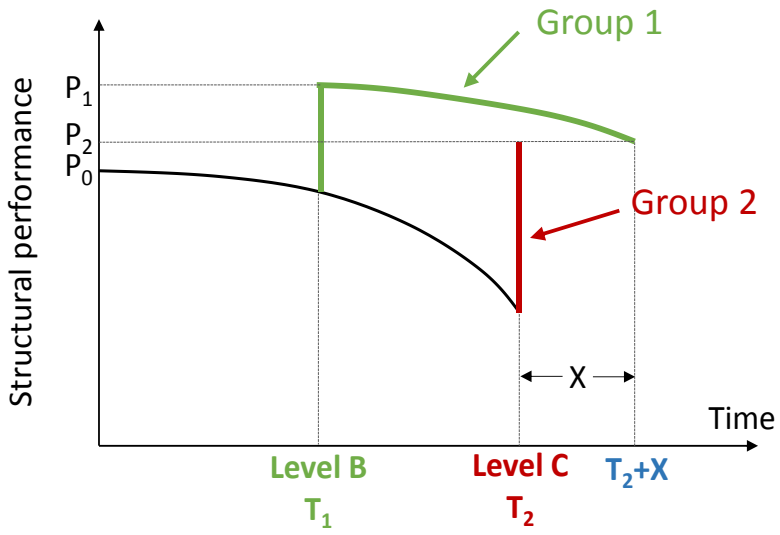

Figure 4.1. Deterioration of structural performance

4.2 LOAD CARRYING CAPACITY

Figure 4.2 and 4.3 present the load carrying capacity of the corroded RC beams repaired with SPCM containing PE fiber with different repair plan. The black line present reduction of load carrying capacity of non-repaired corroded beams.

As shown in Figure 4.2, the beams repaired with method 2, when continued second accelerated corrosion, the corrosion process progressed rapidly because the splitting cracks on the beams repaired with method 2 were not fully restored. Therefore, the corrosive agents such as chloride, moisture and oxygen easily penetrated through these cracks which resulted in high corrosion rate. As illustrated in Figure 4.2 and 4.3, load carrying capacity of the beams in group 1 or early repair is higher than those in group 2 or late repair. The improvement of load carrying capacity of the beams in group 1 after the second time accelerated corrosion might be explained by following reasons:

1. Rust product formed again and increased the surface roughness of reinforcing steel which results in improving holding capacity of steel bar. As repair method 3, the concrete surrounding tensile steel was removed all and replaced with SPCM, therefore, this method is more affected by this phenomena, as shown in Figure 4.3.
2. The corrosion occurred in steel bars of the beams in group 1 was more uniform than that occurred in group 2, non-uniform dimension of the steel bar cross-section can be seen in Figure 4.4. This is because when the corroded beams were repaired, leftover corrosive agents were removed, and the damaged concrete and splitting cracks were restored. After repair, moisture, oxygen and dangerous substance ingresses difficulty, that result in stopping localized corrosion.

The localized reduction of steel bar directly affect the structural behavior and performance of RC structure. Load carrying capacity, stiffness and ductility of RC beam will be reduced with increase in beam deflection. The splitting cracks reduce bond strength between concrete and reinforcement and are dangerous to the ductility, fatigue strength and load carrying capacity of the RC beam.

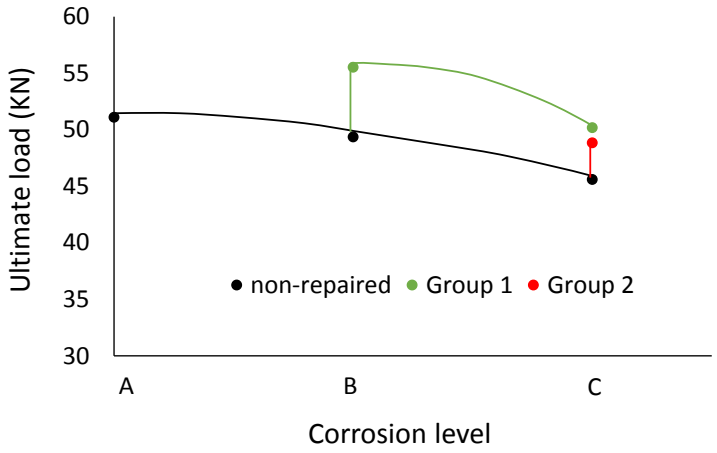

Figure 4.2: Load carrying capacity of the beams repaired with method 2

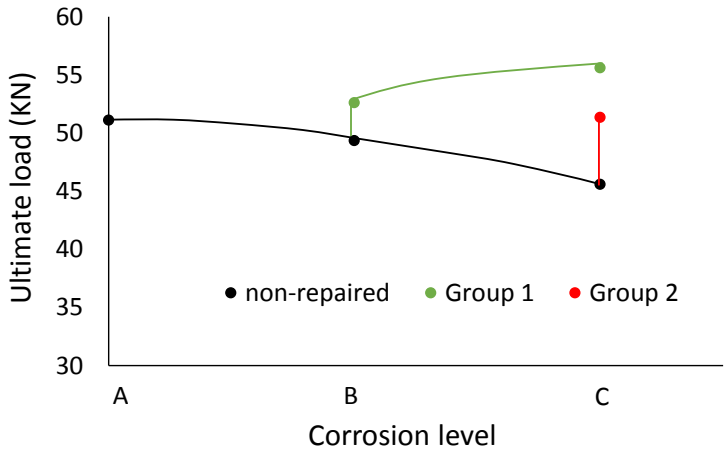

Figure 4.3: Load carrying capacity of the beams repaired with method 3

(a) Steel bar corrosion for the beams in group 1

(b) Steel bar corrosion for the beams in group 2

Figure 4.4: Corrosion of steel bars

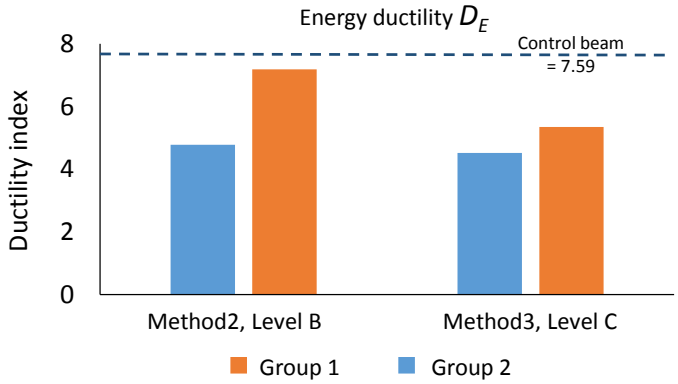

Figure 4.5: Energy ductility

4.3 ENERGY DUCTILITY

The energy ductility indices of the beams in group 1 which were corroded two times are higher than those in group 2, as shown in Figure 4.5. The localized corrosion of the steel bar reduces its load carrying capacity and results in the reduction of the performance such as ductility and flexural stiffness of the overall reinforced concrete member where the corroded steel is contained. Therefore, the reduction in ductility of the repaired beams in group 2 might be the result of localized corrosion of the steel bars.

4.4 FLEXURAL STIFFNESS

The load-average midspan deflection curves of the beams repaired with method 2 and 3 are shown in Figure 4.6 and 4.7, respectively.
The results show that the flexural stiffness of the beams repaired in group 1 is higher than that of the repaired beams in group 2.

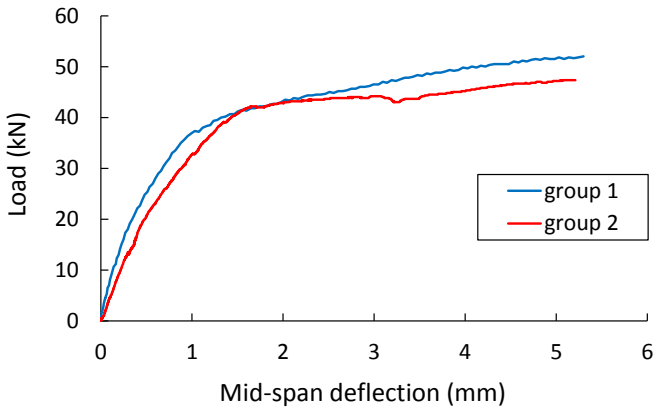

Figure 4.6: Load vs mid-span deflection of the beams repaired with method 2

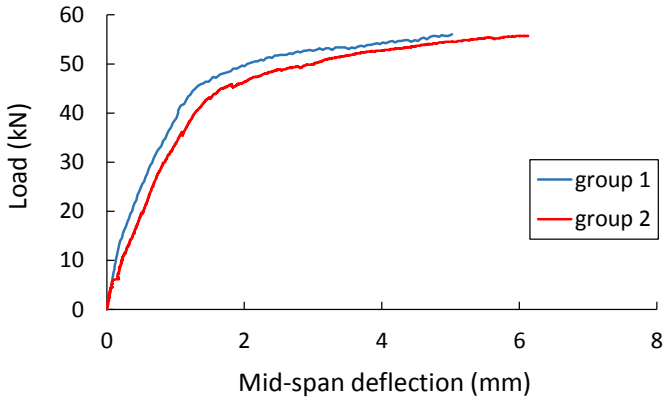

Figure 4.7: Load vs mid-span deflection of the beams repaired with method 3

4.5 CRACK FORMATION

Figure 4.8 – 4.9 present corrosion crack formation of the beams in group 1 after repair and after finish second time accelerated corrosion. For the beams repaired with method 2, large splitting cracks were observed after finish second accelerated corrosion, as shown in Figure 4.8. In this method, the splitting cracks were not fully restored, therefore, corrosion product easily exerted large pressure on these existing cracks, thus these cracks were enlarged (Figure 4.8 (c)). In contrast, for the beams repaired with method 3, splitting cracks were restored and rarely observed on the beam surface after second accelerated corrosion, as shown in Figure 4.9.

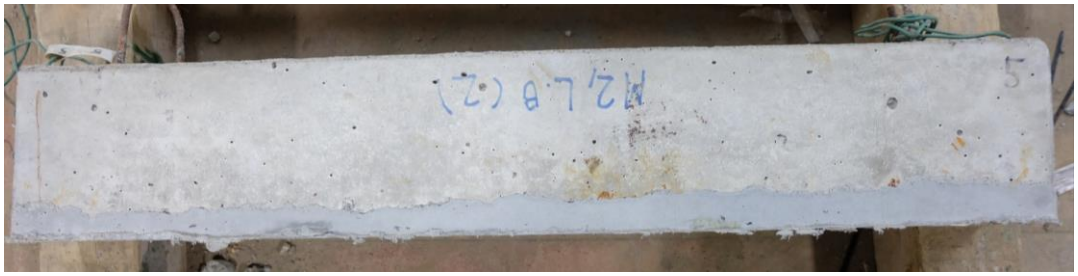

(a) After finish corrosion for the first time and then the beams were repaired with method 2

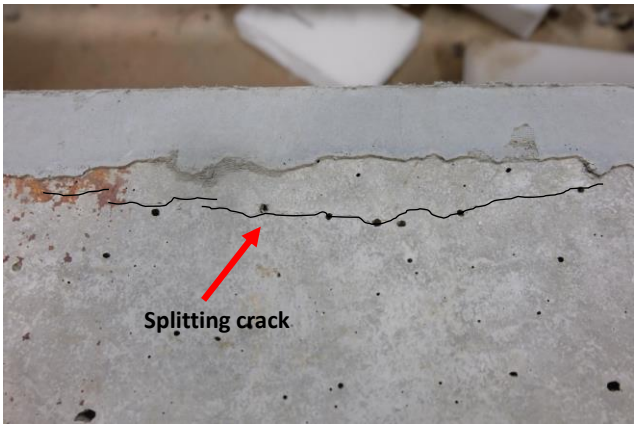

(b) Splitting crack was not fully stored

(c) After finish corrosion for the second time

Figure 4.8: Crack formation of the beams repaired with method 2

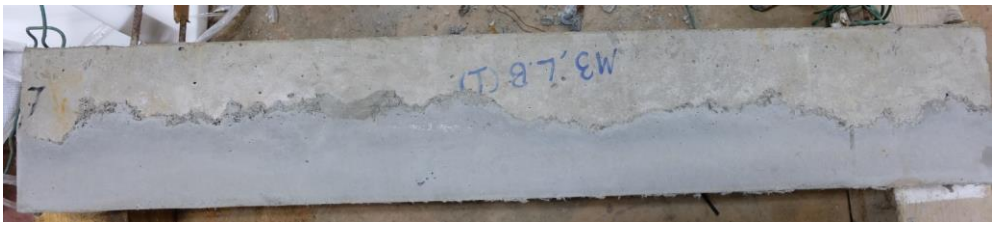

(a) After finish corrosion for the first time and then the beams were repaired with method 3

(b) After finish corrosion for the second time

(c) Corrosion crack after finish second accelerated corrosion

Figure 4.9: Crack formation of the beams repaired with method 3

Figure 4.10 (a) and (b) present crack formation of the corroded beams in group 1 repaired with method 2 and 3, respectively, when conducting four point bending tests. Crack formation of the beams in group 1 are similar to the beams in group 2 as presented in Chapter 3. For the beams repaired with method 2, first the flexure cracks formed followed by concrete or SPCM peeling at the mid-span area, as shown in Figure 4.10 (a), the details of this kind of crack formation are explained in Chapter 3. In case of the beams repaired with method 3, flexural cracks were observed accompanied by concrete crushing in the compression zone (Figure 4.10 (b)).

(a) The beam repaired with method 2

(b) The beam repaired with method 3

Figure 4.10: Crack formation of the beams in group 1 after bending test

4.6 SUMMARY

From this case study it was found that, maintenance or repair plan is a major concern in designing of durability.

The beams were done with late repair lead to localized corrosion of the steel bar, which reduces its load carrying capacity and results in the reduction of the performance of the overall RC beams. Load carrying capacity, flexural stiffness and ductility of repaired beams reduced with the increase in average midspan deflection. Furthermore, service life of the beams repaired with method 2 is shorter than those repaired with method 3. In method 3, the lost bond between tensile steel and concrete is fully restored, the leftover corrosive agents are removed, and splitting cracks are recovered. In contrast, for method 2, the lost bond and splitting cracks are not fully restored, and there are some leftover corrosive agents in concrete over tensile reinforcement.

It should be put in mind that there is no concrete structure that will last forever without needs of repair and maintenance. The beams shall be done repair or maintenance at the right time, not too early nor too late, because a good maintenance plan will prolong the service life of the structure as well as beneficial in terms of economic.

CHAPTER 5

CONCLUSIONS AND FUTURE WORKS

5.1 CONCLUSIONS

In this study, the effectiveness and potential of using waste fishing nets as recycled nylon fiber to reinforce mortar were experimentally tested and discussed. It can be proposed the use of nylon short fiber recycled from waste fishing nets improves mechanical properties of mortar. Compressive and three-point bending tests were performed to investigate compressive strength, peak load, flexural strength, toughness indices and residual strength factors. The results of the investigation demonstrated the reasonable mechanical properties of reinforced mortar with recycled nylon fiber. A possible way to recycle waste fishing nets as a mortar reinforcing material can be found.

The following conclusions can be drawn:

- The addition of recycled nylon fiber, whether straight or knotted, results in a reduction in mortar workability. However, if considering at 1% of volume fraction of recycled nylon fiber, the mixes that contain knotted fiber present larger flowability. As consideration for the same fiber fraction, the mixes with PVA fiber afford less flow diameter than other types of fiber at the same fiber fraction and a similar fiber aspect ratio.
- The addition of every type of fiber results in a decrease in compressive strength of mortar because of the low Young's modulus of the fiber. Moreover, the compressive strengths are observed to be lower with higher fiber fraction and longer fibers. The addition of knotted fiber leads to reductions in compressive strength of 14-44%.
- The flexural strengths of KN and SN mortar are increased by up to 22-41%. However, if comparing flexural strengths with a 1% fiber fraction, the flexural strength of KN mortar is 37% lower than that of SN mortar. The plain mortar exhibits sudden failure as soon as its stress reaches its peak, while the fiber reinforced mortar sustains stress even less than the peak value with increase in deformation.
- The addition of fiber affords a more ductile mode of failure, which leads to an increase in the load carrying capacity of fiber reinforced mortar. The post peak load is observed to be higher for higher fiber fractions and longer fibers.
- The characteristics of fiber such as diameter, length, geometrical shape, tensile strength and Young's modulus as well as bond between the fiber and cement matrix, directly affect the post peak behavior, toughness and residual strength of fiber reinforced mortar. Toughness and residual strength of fiber reinforced mortar are dependent on such the characteristics of fiber. The R-nylon fiber used in this study has smooth surface, which lead to poor frictional resistance between fiber and matrix. On the other hand, PET fiber has embossed surface, which significantly enhance the post peak load carrying capacity. In addition, as evidenced by the results, the longer fiber improves more toughness and residual strength due to better stress transferring from matrix to fiber.
- The use of knotted fiber is not practical because the fiber tends to form fiber balls and it is difficult to control the fiber orientation. Therefore, the fiber fraction should be limited to use in low, and as a result, it is difficult to ensure its effectiveness on the mechanical

properties of fiber reinforced mortar.

It must be noted, however, that the R-Nylon fiber reinforced mortars analyzed in this study have been proven beneficial in terms of flexural strength, material toughness and residual strength as virgin fiber, even if a higher fiber fraction may be required to match the performance of virgin fiber reinforced mortars. Additionally, the use of waste fishing nets as recycled nylon fiber results in an environmental beneficial effect. The recycled straight nylon and recycled knotted nylon fibers used in this study were cut by hand while the R-PET and PVA fibers have been thoroughly treated by industrial manufactures.

Moreover, in this thesis, an experimental investigation was conducted on the use of SPCM for repairing corrosion-damaged beams. The effects of mixing R-nylon fiber into SPCM on the repair effectiveness was investigated in comparison with two common SPCM types: plain SPCM without fiber and SPCM with PE fiber. The following conclusions can be drawn.

- The beams repaired with fiber-containing SPCM, especially PE fiber, showed higher stiffness than those repaired with non-fiber SPCM. Furthermore, the beams repaired with R-nylon fiber-containing SPCM provided ductility that was both excellent and superior to the other SPCM types as well as to non-damaged RC beams.
- As evidenced by experimental studies, SPCM types and repair methods play an important role in the crack formation of the repaired RC beams. Number of severe cracks were found to be higher when using non-fiber SPCM.
- As evident by three point bending test results, the load carrying capacity of R-PET fiber reinforced mortar was significantly enhanced after the peak load due to the mechanical anchorage effect in the embossed surface. Addition of R-PET fiber to SPCM to repair the corrosion damaged RC beam would be expected to significantly improve the load carrying capacity, especially ductility.
- Removal of concrete to a depth of 10 mm deep in combination with SPCM containing PE fiber is suitable for strengthening new RC beams to prolong their service life. For the beams that have lost less than 10% of their tensile steel mass, repair method 2, in which the whole concrete covering is removed, is suitable for improving performance and can be a better choice in terms of economics. However, method 3 which the concrete be removed to a depth of 20 mm beyond the tensile reinforcement in combination with SPCM containing PE fiber, also can restore structural performance and prolong service life of RC beam longer than method 2 by protecting steel against further corrosion. Based on the experimental results, it is recommended that, for beams whose mass loss of tensile steel is 10% to 18%, repair method 3 in combination with SPCM containing fibers. Especially, this repaired depth in combination with SPCM containing R-nylon fiber exhibited excellent improvement of load carrying capacity, flexural stiffness, and especially ductility that was superior to all SPCM types as well as non-damaged RC beams. It is noted that for the beams having mass loss of tensile steel more than 18%, only replacement with SPCM is not sufficient for load carrying capacity recover.

5.2 FUTURE WORKS

This research is expected to contribute to guidelines for sprayed polymer cement mortar repairs to corrosion-damaged RC beams under service loads. Moreover, the investigation of using

recycled nylon fiber was successfully concluded.

For two common types of SPCM, which are polyethylene fiber SPCM and plain SPCM (without fiber), were also investigated in order to compare efficiency to SPCM mixed with the R-nylon fiber. In addition, three repair specifications were focused: removal to a depth of 10 mm, removal of all cover concrete, and removal to a depth of 20 mm over the tensile reinforcements. Four point bending tests were conducted. The results showed that the stiffness of repaired RC beams was found significant improvement, especially using SPCM containing PE fiber. However, loss of ductility has been found after repaired with SPCM containing PE fiber. In case of the beams repaired with SPCM containing R-nylon fiber, they exhibited excellent ductility indices, and these were the best of any SPCM type. Therefore, more research on fiber reinforced polymer cement mortar should be carried out towards maximizing the repair effectiveness of structural repair as follows:

- To maximize the repair effectiveness, two different size of fiber are combined to improve the structural performance of repaired RC beams with SPCM, as illustrated in Figure 5.1. According to small size of PE fiber, the fiber play important part in delaying the formation of a through-specimen macro-crack which results in improvement of pre-peak mechanical performance. In case of R-nylon fiber, according to greater length and diameter, which is effective at bridging macro-cracks and imparting ductility to the composite.

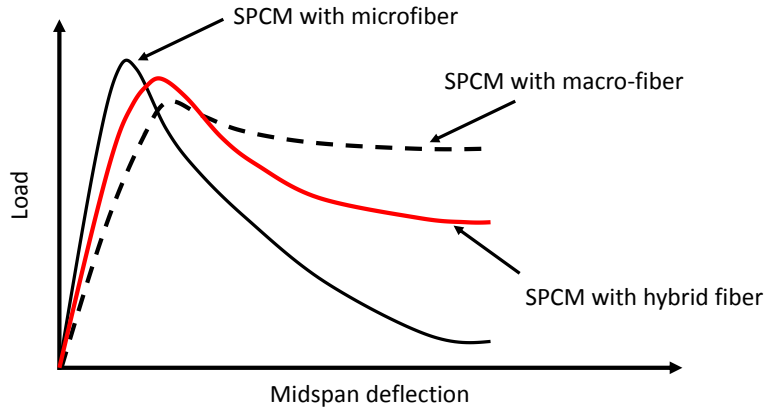

Figure 5.1: Typical load vs deflection curves for the fiber reinforced mortar

- In this study, the load carrying capacity of the repaired beams having mass loss of tensile steel more than 18%, only replacement with SPCM is not sufficient for load carrying capacity recovery. Therefore, combined repair technique should be carried out to improve repair effectiveness.
- Structural performance of corrosion damaged RC beam repaired with R-PET fiber containing SPCM should be investigated and compare repair effectiveness with R-nylon fiber containing SPCM.